

VARIABLE STARS OBSERVED IN THE GALACTIC DISK BY AST3-1 FROM DOME A, ANTARCTICA

LINGZHI WANG^{1,2,3}, BIN MA^{1,3}, GANG LI⁴, YI HU^{1,3}, JIANNING FU⁴, LIFAN WANG^{3,5,6}, MICHAEL C. B. ASHLEY⁷, XIANGQUN CUI^{3,8}, FUJIA DU^{3,8}, XUEFEI GONG^{3,8}, XIAOYAN LI^{3,8}, ZHENGYANG LI^{3,8}, QIANG LIU^{1,3}, CARL R. PENNYPACKER⁹, ZHAOHUI SHANG^{1,3,10}, XIANGYAN YUAN^{3,8}, DONALD G. YORK¹¹, JILIN ZHOU^{3,12}

Draft version April 6, 2024

ABSTRACT

AST3-1 is the second-generation wide-field optical photometric telescope dedicated to time domain astronomy at Dome A, Antarctica. Here we present the results of *i* band images survey from AST3-1 towards one Galactic disk field. Based on time-series photometry of 92,583 stars, 560 variable stars were detected with *i* magnitude ≤ 16.5 mag during eight days of observations; 339 of these are previously unknown variables. We tentatively classify the 560 variables as 285 eclipsing binaries (EW, EB, EA), 27 pulsating variable stars (δ Scuti, γ Doradus, δ Cephei variable and RR Lyrae stars) and 248 other types of variables (unclassified periodic, multi-periodic and aperiodic variable stars). Among the eclipsing binaries, 34 show O'Connell effects. One of the aperiodic variables shows a plateau light curve and another one shows a secondary maximum after peak brightness. We also detected a complex binary system with RS CVn-like light curve morphology; this object is being followed-up spectroscopically using the Gemini South telescope.

Subject headings: astronomical sites: Dome A – photometry: variable stars

1. INTRODUCTION

Time domain astronomy is the investigation of astronomical objects as a function of time, and has long been a source of interesting and unexpected discoveries. On-going and new ground- and space-based large synoptic sky surveys, such as the (intermediate) Palomar Transient Factory (Law et al. 2009; Rau et al. 2009), the SkyMapper Telescope (Keller et al. 2007), and the Large Synoptic Survey Telescope (LSST Science Collaboration et al. 2009) after its first light in 2020¹³, are exploring or will explore new regions of parameter space in terms of depth and temporal coverage.

The Antarctic plateau offers a number of unique advantages for precision, ground-based, time-domain as-

tronomy, such as the ability to observe continuously during winter, low scintillation noise, excellent seeing above a very low boundary layer, low airmass variations, low aerosols, low water vapor, more stable atmospheric transmission, wider wavelength windows, and a dark sky in the infrared (Lawrence et al. 2004, 2006, 2008; Moore et al. 2008; Kulesa et al. 2008; Aristidi et al. 2009; Burton 2010; Zou et al. 2010; Yang et al. 2010; Sims et al. 2010; Bonner et al. 2010; Lascaux et al. 2011; Tremblin et al. 2011; Pei et al. 2011, 2012; Sims et al. 2012a,b; Giordano et al. 2012; Storey 2013; Hu et al. 2014; Ashley 2013; Yang et al. 2016). There is thus considerable interest in overcoming the technical challenges of operating in Antarctica, so that the advantages for astronomy can be realized (Tothill et al. 2008; Kulesa et al. 2008; Crouzet et al. 2010; Chapellier et al. 2016; Mékarnia et al. 2016).

Dome A (latitude 80°22'02"S, longitude 77°21'11"E, elevation 4093m above the sea level) is the highest region on the Antarctic plateau and is being used for a series of three increasingly ambitious optical survey telescopes (Yang et al. 2009; Gong et al. 2010). The first optical telescope was called CSTAR (the Chinese Small Telescope ARray; Yuan et al. 2008) with an effective aperture of 10 cm and field of view (FOV) of 20 deg² and was installed at Dome A in January 2008; CSTAR produced a 3-year photometric dataset, and a number of studies of stellar variability have been published (Zhou et al. 2010a,b; Wang et al. 2011, 2012; Zhou et al. 2013; Wang et al. 2013a,b; Meng et al. 2013; Huang et al. 2013; Fu et al. 2014; Qian et al. 2014; Wang et al. 2014a,b; Zong et al. 2015; Huang et al. 2015; Wang et al. 2015; Yang et al. 2015; Oelkers et al. 2015, 2016; Liang et al. 2016). The second-generation of optical telescope at Dome A is called AST3, which in turn consists of three telescopes, each with an entrance pupil diameter of 0.5 m, and a FOV of 4.3 deg² (Cui et al. 2008; Yuan & Su 2012; Yuan et al. 2014, 2015). The first

¹ National Astronomical Observatories, Chinese Academy of Sciences, Beijing 100012, China. wanglingzhi@bao.ac.cn

² Chinese Academy of Sciences South America Center for Astronomy, Camino EL Observatorio 1515, Las Condes, Santiago, Chile

³ Chinese Center for Antarctic Astronomy, Nanjing 210008, China

⁴ Department of Astronomy, Beijing Normal University, Beijing, 100875, China

⁵ Purple Mountain Observatory, Chinese Academy of Sciences, Nanjing 210008, China

⁶ Mitchell Institute for Fundamental Physics & Astronomy, Department of Physics & Astronomy, Texas A&M University, College Station, TX 77843, USA

⁷ School of Physics, University of New South Wales, NSW 2052, Australia

⁸ Nanjing Institute of Astronomical Optics and Technology, Nanjing 210042, China

⁹ Center for Astrophysics, Lawrence Berkeley National Laboratory, Berkeley, CA, USA

¹⁰ Tianjin Normal University, Tianjin 300074, China

¹¹ Department of Astronomy and Astrophysics and Enrico Fermi Institute, University of Chicago, Chicago, IL 60637, USA

¹² School of Astronomy and Space Science and Key Laboratory of Modern Astronomy and Astrophysics in Ministry of Education, Nanjing University, Nanjing 210093, China

¹³ <https://www.lsst.org/about/timeline>

two of the AST3 telescopes—AST3-1 (Li et al. 2012a,b; Wen et al. 2012) and AST3-2—were installed at Dome A in January 2012 and 2015, respectively. The third AST3 telescope is planned to be installed in 2017, and will have a K-band infrared camera. The third-generation optical/infrared telescope destined for Dome A is called KDUST (the Kunlun Dark Universe Survey Telescope; Jia & Zhang 2012, 2013; Yuan et al. 2013; Zhu et al. 2014; Burton et al. 2016; Li et al. 2016; Xu et al. 2016), which has an aperture of 2.5 m and FOV of $\sim 2.3 \text{ deg}^2$ (Yuan et al. 2013); KDUST is expected to be operational at Dome A after 2022.

The three AST3 telescopes were originally conceived as multi-band survey telescopes, with each telescope having a fixed filter to reduce the risk of mechanism failure. Their main sky survey area is a zenith distance less than 70° (Yuan & Su 2012). Meanwhile, other factors for observations are also taken into account, including the altitude and phase of the Moon, the angular distance between the telescope pointing and the Moon, and the altitude of the Sun (Shang et al. 2012). To operate the AST3 at remote Dome A, an improved version of PLATO (an automated observatory platform for CSTAR and other earlier instruments¹⁴), PLATO-A was designed to offer about 1 kW power source for AST3 (Lawrence et al. 2009; Ashley et al. 2010; Shang et al. 2012).

The three main science goals for AST3 are the early detection of supernovae, exo-planet transit searches, and stellar variability (Cui et al. 2008). The first AST3 telescope (AST3-1) was deployed to Dome A in January 2012 successfully and $\sim 16,000$ scientific frames were collected from March 16 to May 7, 2012, with a total exposure time of 189 hours. After that, AST3-1 unfortunately stopped work due to a malfunction a power distribution box. Of the $\sim 16,000$ images obtained, 4,000 were of 500 fields mainly surveyed for supernova templates; ~ 4700 images were of the center of the Large Magellanic Cloud, and ~ 3400 images covered eight Galactic disk fields to study Wolf-Rayet stars, and one Galactic disk field was used primarily to search for transiting exo-planets. This latter field had the most number of observations, and so was also suited to a study of stellar variability, which is the subject of this paper. The field was centered at $l = 289.6347^\circ$, $b = -1.5718^\circ$, and was monitored in i band with 3523 images over 8 days with a total exposure time of 38.9 hours. Of these 38.9 hours, 157 frames totalling 2.6 hours were observed on March 28, and 3366 frames totalling 36.3 hours were from April 24 to May 1 (Table 1). The distribution of the 36.3 hours over the 7 days of observations can be seen from the time-series plots. Gaps in the observations were mainly due to the AST3-1 telescope being pointed to other fields. The observations, the data reduction, and the time-series photometry are briefly described in §2. The catalog of variable stars and preliminary statistics of the variable star types are presented in §3. Our results are summarized in §4.

2. OBSERVATIONS AND DATA REDUCTION

2.1. Observations

TABLE 1
LOG OF OBSERVATIONS

Date 2012	# images	Total exp. time (hr)
3-28	156	2.56
4-24	6	0.02
4-25	515	6.91
4-26	516	6.03
4-27	58	0.83
4-28	368	5.64
4-29	666	6.55
4-30	750	6.25
5-01	488	4.07
Total	3523	38.86

AST3 (Cui et al. 2008; Yuan et al. 2014, 2015) was conceived as three telescopes, each equipped with one of three SDSS g , r and i filters. Each telescope has an entrance pupil aperture of 0.5 m and a wide FOV of 4.3 deg^2 , and is equipped with a $10\text{K} \times 10\text{K}$ frame transfer STA1600FT CCD (Charge Coupled Device) camera. The CCD detector is divided into frame store regions at the top and bottom quarters and an image area in the central half in order to operate in frame transfer mode without a shutter—this is part of our risk-mitigation strategy of eliminating mechanisms as far as possible, since the telescope has to operate entirely remotely for 11 months of the year with no possibility of repairs being carried out. The image area of the CCD has 16 readouts, each with 1320×2640 pixels, including an overscan region of 180 columns on the readout electronics end. More details about the AST3 CCD performance, data system and survey strategy can be found in Ma et al. (2012); Shang et al. (2012); Z. Shang et al. (2016, in preparation); Q. Liu et al. (2016, in preparation). For the total of 3523 images obtained of our field, 65% had exposure times of 30 seconds, and the remainder were 60 seconds. The field is not crowded as the median distance between every star and its nearest neighbor from our reference frame is 11.14 pixels (note that the AST3-1 pixel scale is 1.0 arcseconds/pixel). The stellar brightness profiles had a median FWHM (full width half maximum) of 3.73 pixels. The low level of crowding led us to use aperture photometry rather than PSF-fitting.

The field probes the Galactic disk center at $l = 289.6347^\circ$, $b = -1.5718^\circ$, which was also monitored by the Optical Gravitational Lensing Experiment (OGLE-III; Fig. 1 of Pietrukowicz et al. 2013). Limited data bandwidth (128kbps for our Iridium OpenPort system; Xu 2012) from Dome A meant that the raw images were carried back from Dome A on hard disk drives by the 29th Chinese Antarctic Research Expedition (CHINARE) team. The satellite bandwidth is sufficient for transferring only small sections of images and highly-reduced data (Shang et al. 2012).

2.2. Data reduction

The preliminary reduction of the raw science images involved crosstalk correction, bias subtraction, dark current subtraction, and flat fielding. The inter-channel interference crosstalk due to the multi-channel CCD readout, was corrected first. Overscan regions of the 16 readouts were used to correct the corresponding bias. Problems with the CCD’s thermoelectric cooler during 2012

¹⁴ <http://mcba11.phys.unsw.edu.au/~plato-a>

meant that the images were subject to high dark current levels, comparable to the sky background. A new method was applied to calculate a dark frame from image pairs. More specifically, our dark frame was derived by combining 230 image pairs (each pair having the same temperature and exposure time), and was scaled to the same temperature and exposure time as the scientific images for dark current correction (Ma et al. 2014).

The flat-fielding of AST3-1’s wide field was achieved in two steps. Due to the relatively large 4.3 deg^2 FOV, a sky brightness gradient of $1\% \sim 10\%$ from individual twilight flat-field image remained after pre-processing for crosstalk, overscan, and dark current. The 200 twilight flat-field images were selected to correct the sky brightness gradient. More specifically, for each of the 200 twilight flat-field images, the brightness gradient was first fitted with an empirical function based on the sun’s altitude, and the angle between the image and the sun. The gradient was removed by dividing each image by the empirical fit, and the resulting 200 twilight images were then median-combined to obtain a master flat field, which was used for flat-fielding corrections for the science images (Wei et al. 2014).

After finishing the preliminary reduction, SExtractor (Bertin & Arnouts 1996) was applied to perform aperture photometry on all the scientific images. The aperture selection with 4 pixels (SExtractor’s MAG_APER parameter) was adopted as it gave the minimum $r.m.s$ photometric uncertainties on a test image (B. Ma et al. 2016, in preparation). The photometric uncertainty reached 2 mmag for bright stars $< 13 \text{ mag}$ on a typical image. In order to obtain accurate astrometry, the photometric results were fed into SCAMP (Bertin 2006) to register the positions of all the images with the PPMX system (Position and Proper Motions eXtended, Röser et al. 2008). Our photometric calibration was divided into two steps. First, a magnitude difference between an individual image and the reference image (the highest quality image) was obtained by matching ~ 1000 bright, isolated stars. Then, stars in the reference image that were also in the APASS (the AAVSO Photometric All-Sky Survey¹⁵) catalog (Henden et al. 2016) were used to adjust the zero point of our magnitudes. APASS is an all-sky photometric survey, conducted in five filters: Johnson B and V, plus Sloan g , r , i bands. The AAVSO (American Association of Variable Star Observer¹⁶) was created by amateur astronomers, and collects and archives variable star observations.

2.3. Time-series photometry

During the 8 days of observations, 3,523 images were collected in total for our field and 96,734 bright stars with $S/N > 30$ were found on our reference image, which had the largest number of detections. We then rejected stars that were detected in fewer than 20% of the images. We are ignoring such objects but they could be interesting. This left a final sample of 92,583 stars.

Fig. 1 displays the $r.m.s$ variations in the light curves of our sample stars as a function of error-weighted magnitude. The magnitude were weighted by their photometric errors after rejecting 3σ outliers iteratively until

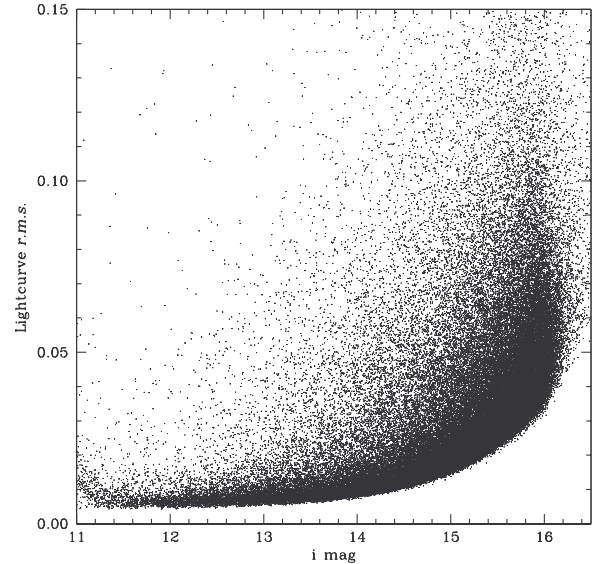


FIG. 1.— $r.m.s$ magnitude range of light curves of 92583 stars with at least 20% measurements.

the maximum iteration reaches 10. The $r.m.s$ is less than 0.02 mag for stars brighter than 15.4 mag. And the $r.m.s$ is less than 0.05 mag when the magnitudes are smaller than 16.4 mag, which accounts for 78% stars in our sample.

The photometric errors estimated by SExtractor were under- or overestimated due to various reasons such as underestimated flat-fielding errors, and less than perfect photometry. We worked around this problem by assuming that the majority of stars are constant and assuming the errors for this majority are roughly Gaussian as the $\chi^2/N_{DOF} = 1$ for the constant stars. Following the reference in Kaluzny et al. (1998), we firstly calculated the χ^2/N_{DOF} value for all the stars and then derived a scale factor curve for constant stars. Then we re-scaled all stars by multiplying by this curve. The re-scaled photometric errors were then used in the calculation of the Welch-Stetson variability index L (Welch & Stetson 1993; Stetson 1996) to find variable candidates for the next section.

3. VARIABLE STAR CATALOG AND STATISTICS

3.1. Searching for Variability

The search for variable stars in our sample was conducted in three steps. Our candidates were initially selected as those stars with statistically significant magnitude variations. Such stars didn’t necessarily show a periodic behavior. Then for the selected candidates we conducted a search for periodic behavior. Finally we used visual inspection of the phase-folded light curve and time-series diagram of each candidate to distinguish periodic and aperiodic variables.

Variable stars exhibit magnitudes variations that can be measured by the Welch-Stetson index (Welch & Stetson 1993), later slightly modified as the L variability index by Stetson (1996). We calculated L for each light curve in our sample using VARTOOLS

¹⁵ <https://www.aavso.org/apass>

¹⁶ <https://www.aavso.org/>

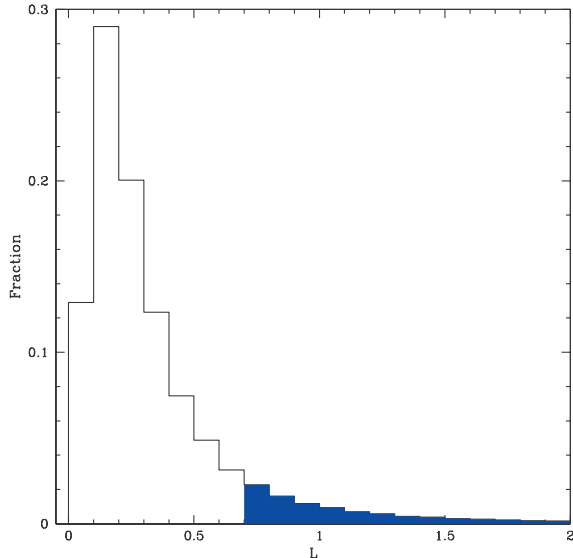


FIG. 2.— Distribution of the Welch-Stetson variability statistic L (Welch & Stetson 1993; Stetson 1996) for the 92,583 brightest stars in the AST3-1 sample.

¹⁷ (Hartman et al. 2008; Hartman & Bakos 2016). The resulting L distribution in our sample is shown in Fig. 2; the overall distribution can be interpreted in terms of two components, one of which – the one presumably corresponding to non-variable stars – resembles a Gaussian, while the other – presumably corresponding to the variables – behaves rather like an exponential tail. We measured a median value of $L = 0.22 \pm 0.17$ for all stars with $L < 0.8$. We used $L \geq 0.65$ (equivalent to a $+2.5\sigma$ selection) as the cut-off for our variable candidates.

We use Lomb-Scargle (Lomb 1976; Scargle 1982, hereinafter LS) and box fitting algorithms (Kovács et al. 2002, hereinafter BLS) to detect the periods of our variable candidates. The LS method applies the statistical properties of least-squares frequency analysis of unequally spaced data on a series of test periods. We hunted for periods between 0.01 and 10 d and applied a bin size of 0.01 d. Periods with $S/N \geq 12$ in the periodogram were taken to be significant. The BLS method searches for signals characterized by a periodic alternation between two discrete levels with much less time spent at the low-level (occultation) phase. Similar methods (LS & BLS) for hunting for variable stars, were applied in Wang et al. (2011, 2013a); Yao et al. (2015). Surveys such as OGLE II use the Detached Eclipsing Binary Light curve fitter (Devor 2005, hereinafter DEBiL) for finding and analyzing eclipsing binaries in large datasets. We also used the DEBiL code to find the corresponding periods of our variable candidates as an independent check of the periods found by the LS and BLS methods. We visually inspected the phased light curve folded by the periods found from each of the LS, BLS and DEBiL methods, and selected the period that had the smallest *r.m.s.*. Due to the very short observing window (only eight days of observations over 34 days) and observing gaps (when AST3-1 was pointing elsewhere, and avoiding twilight),

we found that in some cases periods produced by the LS, BLS or DEBiL methods did not produce well-folded phase curves. In these cases we manually adjusted the period to produce the best result.

In order to calculate the uncertainty of the above derived periods, we ran Markov Chain Monte Carlo (MCMC; Brooks 1998) simulations of the high-order harmonic function as given in equation (1),

$$F(t) = a_0 + \sum_{i=1}^{12} \left[a_i \sin\left(\frac{2\pi ti}{P}\right) + b_i \cos\left(\frac{2\pi ti}{P}\right) \right] \quad (1)$$

based on the detected period using the *-nonlinfit* tool of VARTOOLS (Hartman & Bakos 2016). We used a 12th order fit to the light curve, which was able to fit eclipsing binaries with relative deep depths. The number of accepted links in a given fit was set to 1000. The initial guess and step size of each a_i and b_i were found by fitting the equation (1) to each light curve with a fixed period. The median value of each period and its uncertainty were calculated in the MCMC simulation by again fitting the equation (1) to each light curve, but now with the constraint $0.01 < P < 8.0$.

Next, we visually inspected the light curve of each variable candidate to search for objects with statistically significant variations in magnitude that did not necessarily show a periodic behavior during our 8-day observations. Our final catalog of variables contains 560 stars in the magnitude range from 10.87 mag to 16.23 mag, 339 of which are new discoveries by AST3-1. Table 2 lists the properties of all the detected variables. Column 1 lists the 2012 AST3 ID; columns 2 and 3 give the right ascension and declination matched to the PPMX system; column 4 contains the weighted mean *i*-band magnitude; column 5 gives the L value; column 6 lists the most significant median period (top left panel in Fig. 3) in the MCMC simulation, and its standard deviation in brackets in unit of 10^{-9} d (when applicable); column 7 specifies the minimum χ^2 per degree of freedom in the MCMC simulation; column 8 gives the peak-to-peak amplitude of variation; column 9 gives the time of the first minimum light contained in our observations (only for the periodic variables); column 10 contains a tentative classification of the variable ¹⁸, where possible; column 11 has additional information, including previous identification of the variable from the all-sky automated survey run by AAVSO (Pojmanski 2005; Watson et al. 2016) or inclusion in the variable stars of OGLE-III (Samus et al. 2009) or the Bochum Survey of the Southern Galactic Disk (Hackstein et al. 2015, hereinafter GDS).

We matched our final catalog of 560 stars with the AAVSO database and GDS catalog, with a matching radius of 15 arcseconds. This initially resulted in 231 variables stars being previously known. There were 116 variable stars in common between our survey and the AAVSO database, and 104 of these had magnitudes in the Cousins’ infra-red *Ic* band (Watson et al. 2016). There are 152 variable stars in common between our catalog and the GDS database with magnitude values in Sloan *r* band; 139 of these also had magnitude measurements in Sloan *i* band (Hackstein et al. 2015), which is

¹⁷ <http://www.astro.princeton.edu/~jhartman/vartools.html>

¹⁸ <http://www.sai.msu.su/gcvs/gcvs/iii/vartype.txt>

similar to our filter. There are 37 variables that appeared in both the AAVSO database and the GDS catalog. We double-checked our initial matching results by measuring the magnitude difference Δmag our observations and Ic (AAVSO) and i (GDS). For the 104 stars in common with the AAVSO database, we measured a median value of $\Delta mag = (i - Ic) = 0.553 \pm 0.316$ and applied 3σ outliers rejection to the Δmag and also required that the Ic magnitude should be less than 16.5 mag to exclude 6 stars (AST11766, 12622, 37735, 64879, 74215 and 89418) from the initial common sample. The i vs. Ic magnitude diagram for the remaining 98 variable stars is shown in the right panel of Fig. 3. We excluded 4 outliers (AST05375, 57964, 71042 and 83522) with the same method applied to the 139 stars common between our catalog and GDS. i vs. r for 148 variables we have in common with GDS is shown in the bottom left panel of Fig. 3; i vs. i for 135 variables is shown in the bottom right panel.

Our final catalog shows that we have rediscovered 221 previously known variable stars; 96 of these are found in both the AAVSO database and the OGLE-III survey (Pietrukowicz et al. 2013); an additional 14 stars were in the AAVSO database but not in the OGLE-III survey; the remaining 111 stars were found in the GDS catalog. Due to our short observing window, we could not determine the periods of three variables: AST13431, 49035, and 83717. In addition, AST43064 and 62877 are listed in the AAVSO database without a period, and all known variables from the GDS catalog had no measurements of their periods until now. The estimated periods for the remaining 105 variables from AST3-1 are highly consistent with those given in the AAVSO database except for five variables: AST31492, 38531, 39901, 59773, and 68860, which have AST3-1 periods that are half of the AAVSO values. Our period detection methods (LS, BLS) are sensitive to detect sine wave or box-like signals. Our periods should be double for binary stars to show the primary and secondary eclipsing light variabilities, i.e., binaries AST38531, 59773 and 68860. While for another two periodic variable stars AST31492 and 39901, we believe our periods are correct (Fig. 4). The final period-period diagram from AST3-1 and AAVSO database is shown in top left panel of Fig. 3.

We classified half of the variables into binaries, 17% of them into δ Scuti, γ Doradus, δ Cephei, RR Lyrae, and unclassified periodic or multiple periodic variables. Due to our short observing window, we could not detect the periods of the one third of the variables that passed our selection as a result of their significant time series variability. Table 3 contains approximate statistics for the different types, if possible. The folded light curves of the representative periodic variables are showed in Figs. 5 - 8, while the representative light curves of aperiodic variables are showed in Fig. 9. The time-series data of all 560 variable stars will be available in machine readable format through the VizieR Online Data Catalog¹⁹.

3.2. Types of variables found by AST3-1

3.2.1. Eclipsing binaries

Eclipsing binaries can be classified into three broad categories based on the shape of their light curves: Algol-

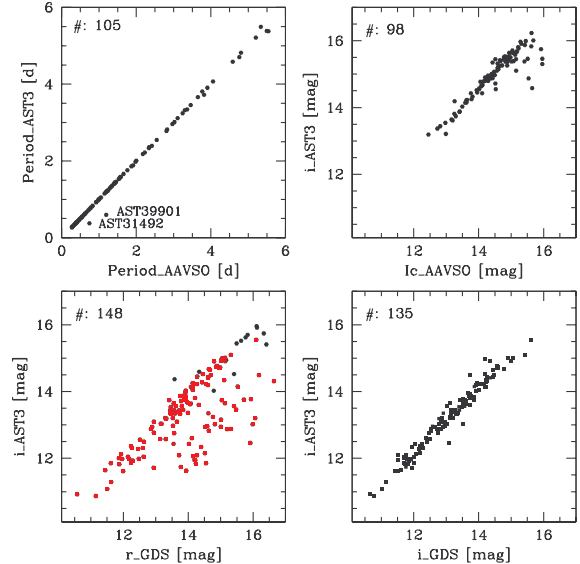


FIG. 3.— Top left: the measured periods for 105 variable stars from AST3-1 compared to the periods given in the AAVSO database; top right: the measured i magnitude for 98 variable stars from AST3-1 compared to the Cousins’ Ic magnitude given in the AAVSO database; bottom left: black solid circles show i magnitude for 148 variable stars from AST3-1 compared to the Sloan r magnitude given in the GDS catalog (red squares for 135 out 148 stars with both r , i band magnitudes); bottom right: i magnitude for 135 variable stars from AST3-1 compared to the Sloan i magnitude given in the GDS catalog.

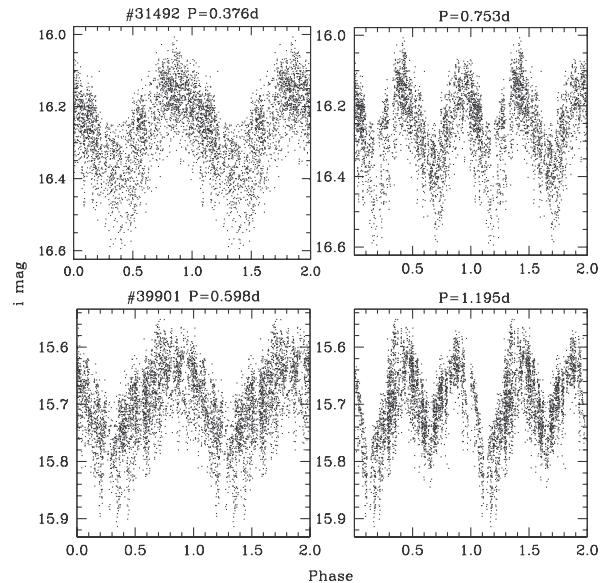


FIG. 4.— Phased light curves were folded by periods from AST3-1 (left panels) and from the AAVSO database (twice that from AST3-1, right panels) for AST31492 and 39901; we believe that the AST3-1 periods are more likely to be correct.

type eclipsing systems (EAs), β Lyrae-type eclipsing systems (EBs) and W Ursae Majoris-type eclipsing variables (EWs). The EA systems have obviously different depths between the primary and secondary minima, and have

¹⁹ <http://vizier.u-strasbg.fr/>

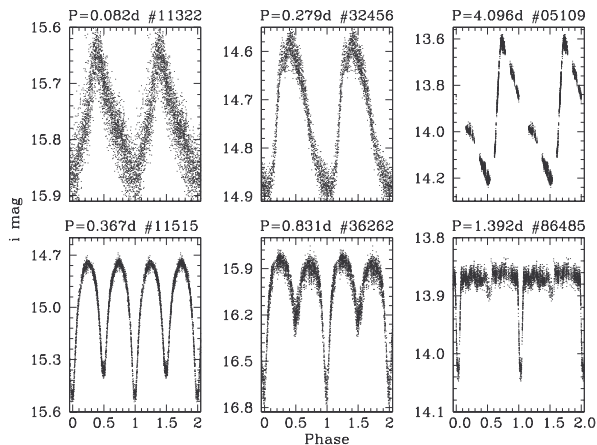


FIG. 5.— Phased light curves for six typical periodic variable stars. The periods and AST IDs are listed above each panel. Top row (from left to right): δ Scuti, RR Lyr c-type star, and δ Cepheid; bottom row (from left to right): eclipsing binaries of W UMa-type (EW), β Lyrae-type (EB), and Algol-type (EA) configurations.

clearly defined times for the beginning and ending of the eclipses; EA systems are often but not always a detached eclipsing system (Catelan & Smith 2015), although the prototype of the class, Algol, is believed to be a semi-detached system (Soderhjelm 1980; Kolbas et al. 2015). The EB systems show a continuous change in brightness and have a deeper primary depth than that of the secondary. The EW systems also show a continuous change in brightness and have an almost equal or non-obvious varying depth between the primary and secondary minima. The EW systems consist of two components almost in contact and thus have periods generally shorter than 1 day. Among our sample, there are 127 EWs, 33 EBs, 138 EAs and 65 stars in question are probably distributed into several different variability classes, including eclipsers, pulsators, and others, which are separated by a pipe symbol “|” in Table 2. In total, we have detected 285 binaries and 143 ones are new detections from our data. Of the 339 new variables, 42% belong to the classes of eclipsing binary stars.

There are 34 interesting EW or EB binaries among our 285 detections which show O’Connell effects, i.e., the two successive out-of-eclipse maxima have unequal height in the light curves (O’Connell 1951; Milone 1968; Nataf et al. 2010). The O’Connell effect can be explained by the interaction of circumstellar material with the binary components (Liu & Yang 2003). The interaction model suggests that the O’Connell effect is most obvious in late type and/or short period binaries. In our sample, a short-period EW binary AST46538 exhibits the most obvious O’Connell effect (Fig. 6), and has a magnitude difference of 0.06 mag in i band between the first and second maximum out-of-eclipse brightness. AST46538 appears in the UCAC4 catalog (Fourth U.S. Naval Observatory CCD Astrograph Catalog; Zacharias et al. 2013) and has $B = 13.697$ mag and $V = 12.916$ mag. It also appears in the 2MASS All-Sky catalog of Point Sources (Cutri et al. 2003) and has J, H, K of 11.311 ± 0.026 , 10.941 ± 0.029 , 10.842 ± 0.027 mag., respectively. In order to estimate the color excess $E(B-V)$ of AST46538, we compared its color-color diagrams ($V-J$ vs. $B-V$,

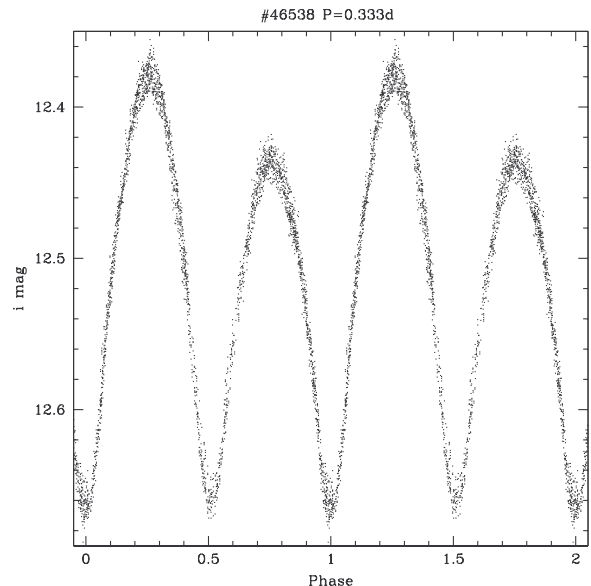


FIG. 6.— The phased diagram of AST46538, which has the most significant O’Connell effect in our sample. Its ID and orbital period are marked in the title.

$V-H$ vs. $B-V$, $V-K$ vs. $B-V$, $J-H$ vs. $B-V$ and $H-K$ vs. $B-V$) with the intrinsic color-color diagrams for main sequence stars²⁰ (Fitzgerald 1970; Ducati et al. 2001) and we found that its interstellar extinction can be neglected. Thus the color term of AST46538 from UCAC4 and 2MASS catalogs can be taken as its intrinsic color to estimate its spectral type, which is equivalent to spectral type G8 (Fitzgerald 1970; Ducati et al. 2001). We find that the spectral type G8 and orbital period 0.333d of AST46538 are close to that of the W UMa binary YY Eri with spectral type G5V and orbital period 0.322d (Liu & Yang 2003); thus, both should exhibit similar O’Connell effects based on the model of Liu & Yang (2003). Indeed, we find consistent O’Connell effects in AST46538 and YY Eri: for YY Eri, the modeled bolometric magnitude difference is 0.07 mag and the observed magnitude difference in V band is 0.04 mag (Liu & Yang 2003), while for AST46538, the observed magnitude difference in i band is 0.06 mag. More observations are needed to double check the above analysis for AST46538.

3.2.2. Pulsating variable stars

Pulsating variable stars exhibit periodic expansion and contraction (radially or non-radially) of their surface layers (Catelan & Smith 2015). The pulsating variable stars are classified into many types based on their period, amplitude, light curve shape, evolutionary status and so on. A more complete classification for all kinds of pulsating variable stars (δ Scuti, γ Doradus, RR Lyrae stars, Cepheids and so on) can be found at Catelan & Smith (2015). δ Scuti variables are late A- and early F-type stars situated in the instability strip on or above the main sequence in the HR Diagram. Their typical pulsation periods are found to be in the range of 0.02d to 0.25 d (Breger 2000). γ Doradus stars locate in the sim-

²⁰ <http://www.stsci.edu/~inr/intrins.html>

ilar position in the instability strip as the δ Scuti stars but with relatively larger pulsating periods ranging from 0.3 d to 3 d (Cuypers et al. 2009). RR Lyrae stars are radially pulsating giant stars with spectral type A to F with periods from ~ 0.2 to ~ 1 d (Smith 2004). Most RR Lyrae stars are pulsating in the radial fundamental mode (RRab stars) and the first overtone mode (RRc stars).

Cepheid variables obey the period-luminosity relation and are divided into two subclasses—type I and type II Cepheids (Catelan & Smith 2015)—based on their masses, ages and evolutionary states. The period-luminosity relation shows that there is a subtype between I and II, called Anomalous Cepheids (Figure 7.3 of Catelan & Smith 2015). The majority of δ Cepheid variables show a large light variation and a rapid rise to maximum and a slow decline back to minimum (i.e., Fig. 7), which is similar to a RR Lyrae star (Schmidt et al. 2004; Soszynski et al. 2008). There are δ Cepheids with lower amplitudes (< 0.5 mag. in V) but they have symmetrical light curves and shorter periods (< 7 days; Catelan & Smith 2015). Type II Cepheids generally shows a relatively broad maximum and a symmetric minimum (Schmidt et al. 2004) and they have periods of ~ 0.8 -35 days and light amplitudes from 0.3 to 1.2 mag in V band ²¹. Anomalous Cepheids show the similar light-curve morphology as RR Lyrae variables with periods shorter than two days and the majority of them show a small bump before the rise to maximum (Soszynski et al. 2008). Based on the light-curve morphology, 12 variable candidates were classified as δ Cepheids as they have higher light amplitudes (> 0.3 mag.), larger periods ($\gtrsim 2$ days) and also exhibit a rapid rise to maximum and a slow decline to minimum. Another 13 variables (AST04480, 09282, 35419, 35518, 40551, 42471, 49241, 53255, 67933, 75631, 79599, 81000, and 84533) also show the morphology of a fast rise and a slow fall, and we have classified them as type “PER” (§3.2.3) since their i amplitudes are less than 0.3 mag. and they have no bumps before the rise to maximum.

In our sample, there are 27 pulsators, which are classified into 10 δ Scuti stars, 2 γ Doradus stars, 12 δ Cepheids, and 3 RR Lyraes. For example, AST13387 is the previously known δ Cepheid GS Car. Its phased light curve in i band can be well fitted by the Fourier decompositions with a fundamental frequency of 0.245616 d^{-1} and the harmonics of 0.497130, 0.736473, 0.984846, 1.225154 d^{-1}) in order of decreasing amplitude values (the red curves in Fig. 7).

3.2.3. Other types of variable stars

For the unclassified 248 variable stars we detected the main periods for 67 of them (periodic and multi-periodic). If the phased light curve folded by its main period was significantly scattered, we classify it as a multi-periodic type variable star, otherwise we classify it as a periodic one. For the remaining 181 unclassified objects we could not detect a period due to the short observing window (8 days spanning 34 days). In our sample, we detected a new complex binary system, AST10442 (Fig. 8). The system has a period of 0.845 d, and an i magnitude of 14.64. The system, which presents RS CVn-like

light curve morphology (obvious variability when out of

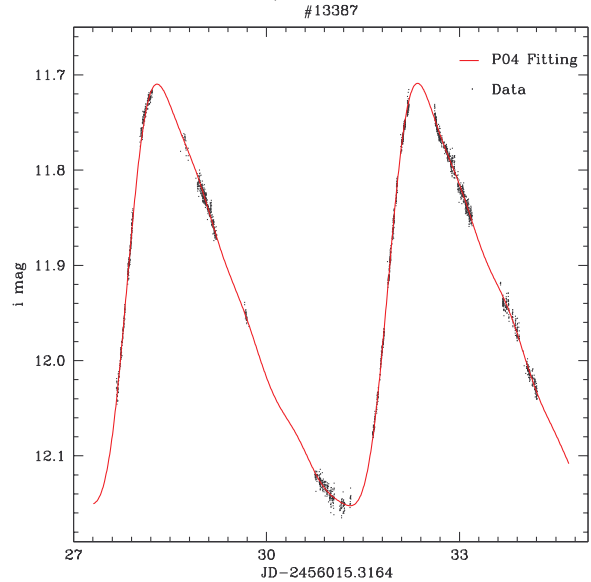


FIG. 7.— Observed light curves of the known δ Cepheid GS Car (AST13387) in i band (black points) and the fitting curves with the fundamental frequency and the harmonics (red curves).

eclipse), shows a primary depth of 0.15 mag but does not show the secondary eclipse on the folded light curve (bottom panel of Fig. 8). AST10442 appears in the SPM4 catalog (Girard et al. 2011) and has $B = 16.59$ mag and $V = 15.24$ mag. It also appears in the 2MASS All-Sky catalog of Point Sources (Cutri et al. 2003) and has J, H, K of $13.254 \pm 0.029, 12.728 \pm 0.022, 12.548 \pm 0.030$ mag., respectively. We have done the same analysis (color-color diagrams) as the AST46538 and found its interstellar extinction can also be neglected. Based on the empirical formula $T_{\text{eff}} = \frac{8540}{(B-V)+0.865}$ (Krishna Swamy 1996; Zong et al. 2015), color $B - V = 1.35$ mag is equivalent to $T_{\text{eff}} \approx 3850$ K. Such low T_{eff} suggests that AST10442 has a spectral type of K5 or M0. If it is a giant, its orbital velocity could be > 500 km/s from Figure 4 of Gaulme et al. (2013). To our knowledge, no published spectroscopic observations have been performed of this interesting system to date. We have obtained 2 hours on Gemini South to carry out spectroscopic observations of this system, in order to measure its maximum radial velocities at phases 0.25 and 0.75.

In addition, out of the 181 aperiodic variable stars, four variable stars AST68688, 40957, 90095 and 83717 with the largest amplitudes in Table 2, are showed in the four panels of Fig. 9. AST68688 and 40957 have shown fast rising variability, i.e., ~ 0.6 mag in 3 days (top panels of Fig. 9). AST90095 shows a brightness plateau during its ascending stage (bottom left panel of Fig. 9); its variability was detected in the GDS catalog, based on sparse data with big gaps (Hackstein et al. 2015). The new variable AST83717 shows a secondary maximum during its descending stage after its i band maximum brightness (bottom right panel of Fig. 9). More observations are needed for further investigations into these four interesting objects.

²¹ <http://www.sai.msu.su/gcvs/gcvs/iii/vartype.txt>

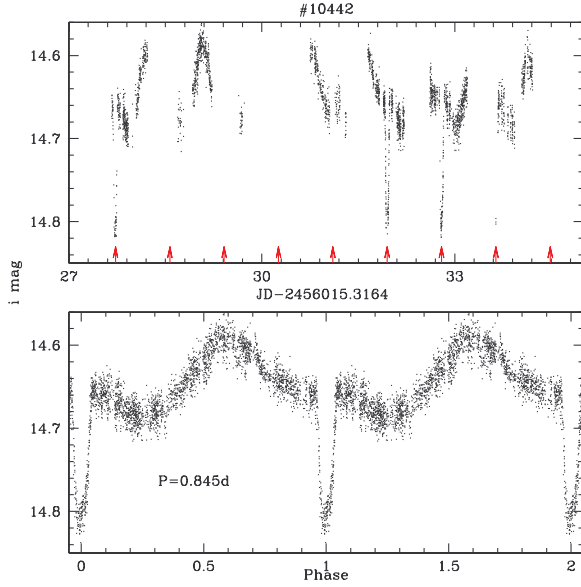


FIG. 8.— Top panel: Light curve of AST10442 in the i band, showing an RS CVn-like pattern with a period of 0.845 d, and a prominent primary minimum clearly detected (marked with arrows in the top plot). Bottom panel: Phased light curve of AST10442 folded by the period of 0.845 d.

TABLE 2
VARIABLE STARS

(1) ID	(2) R.A.	(3) Dec.	(4) i (mag ^a)	(5) L	(6) Period ^b (d)	(7) χ^2	(8) Amp (mag)	(9) T_0^c	(10) Type ^d	(11) Note ^e
AST00006	10:50:18.48	-61:50:54.4	15.31	0.88	0.15	...	VAR	...
AST00391	10:50:21.84	-62:11:29.2	14.71	6.99	3.024214983 (144)	0.48	0.59	...	DCEP	...
AST00424	10:50:20.62	-62:01:08.1	13.13	0.67	2.455793858 (602)	0.26	0.04	15429.813526	EW-OC PER	...
AST00626	10:50:23.52	-62:00:18.8	14.56	1.47	2.310849190 (88)	0.63	0.24	15430.484424	EA	...
AST00651	10:50:23.85	-62:27:13.9	14.35	0.86	0.13	...	VAR	...
AST00723	10:50:20.70	-62:17:13.6	12.90	4.76	0.23	...	VAR	...
AST00769	10:50:25.00	-62:10:13.5	15.21	1.20	0.17	...	VAR	...
AST01150	10:50:27.04	-62:47:05.8	13.84	1.33	1.342747211 (118)	0.32	0.08	15428.847705	EW-OC	...
AST01289	10:50:27.57	-61:59:12.4	13.11	0.75	1.351890564 (204)	0.31	0.05	...	PER	...
AST01361	10:50:28.59	-62:27:36.5	14.95	0.85	0.324106067 (18)	0.98	0.08	15428.167041	PER	...
AST01736	10:50:30.38	-61:35:26.4	14.05	3.65	1.333363891 (38)	0.41	0.23	15429.029346	EB	[G]
AST01935	10:50:29.32	-60:49:45.8	13.77	0.73	2.421975374 (431)	0.40	0.05	15430.448291	PER	...
AST02020	10:50:34.97	-61:59:27.7	15.89	0.95	0.323549092 (17)	0.79	0.15	15428.327198	PER	...
AST02031	10:50:33.64	-62:51:31.4	13.75	1.02	0.103944004 (2)	1.73	0.05	15427.918994	DS	...
AST02065	10:50:34.09	-62:31:19.2	13.74	1.77	0.11	...	VAR	...
AST02152	10:50:34.08	-60:08:33.7	15.53	1.35	0.740864873 (71)	0.52	0.17	15456.359893	PER	...
AST02184	10:50:29.85	-60:13:04.0	12.76	0.87	2.310723543 (310)	0.36	0.07	15456.825713	MP	...
AST02246	10:50:33.77	-60:34:06.7	13.86	1.60	1.058485031 (96)	0.49	0.07	15429.240804	PER	...
AST02460	10:50:34.22	-61:11:10.8	12.41	2.46	0.30	...	VAR	...
AST02497	10:50:36.12	-61:26:00.7	14.58	1.25	0.279432029 (5)	0.68	0.09	15428.068929	EW	[A,O]
AST02664	10:50:36.09	-61:21:30.5	14.38	1.09	0.131989017 (3)	1.30	0.06	15427.890674	DS	...
AST03058	10:50:40.89	-62:03:31.2	15.60	1.06	0.682276845 (35)	0.77	0.20	15428.034180	EW PER	...
AST03182	10:50:41.41	-61:11:20.5	15.39	2.88	0.987051964 (26)	1.65	0.36	15429.252979	EB EW	[A,O]
AST03318	10:50:38.07	-60:45:36.5	12.61	1.03	0.07	...	VAR	...
AST03552	10:50:44.37	-62:03:51.5	14.11	0.81	4.132096767 (1626)	0.36	0.06	15432.010791	PER	...
AST03868	10:50:48.72	-62:30:26.5	15.73	1.20	0.868575275 (21)	0.69	0.44	15428.344776	EA	...
AST04458	10:50:49.81	-60:53:39.9	14.52	1.47	0.09	...	VAR	...
AST04480	10:50:47.56	-61:04:14.7	12.47	0.75	3.719808578 (1112)	0.21	0.05	15433.159750	PER	...
AST04554	10:50:52.64	-61:58:47.2	14.75	3.47	3.075015306 (104)	0.36	0.52	15430.994190	EB	[G]
AST05016	10:50:46.30	-60:28:41.2	11.61	1.03	3.182297707 (582)	0.10	0.13	15432.733448	EW PER	[G]
AST05109	10:50:55.93	-62:05:52.8	13.92	16.22	4.095854759 (137)	0.78	0.61	...	DCEP	...
AST05115	10:50:54.93	-61:29:51.5	13.55	0.90	0.06	...	VAR	...
AST05375	10:50:54.82	-60:21:08.3	12.83	2.25	0.16	...	VAR	...
AST05512	10:50:59.14	-61:09:36.4	15.77	1.02	0.488956094 (11)	0.52	0.39	15428.115283	EA	[A,O]
AST06124	10:51:03.02	-62:18:27.3	12.39	1.17	0.08	...	VAR	...
AST06200	10:51:06.66	-62:33:13.6	14.64	3.34	0.680435836 (8)	7.94	0.36	15428.026416	EA	...
AST06223	10:51:01.75	-61:30:45.9	13.28	1.00	1.355532765 (115)	0.63	0.06	15428.845752	EW PER	...
AST06264	10:51:04.53	-61:21:47.1	14.43	6.17	0.780832171 (9)	0.37	0.36	15428.401416	EW-OC	[A,O,G]

TABLE 2 — *Continued*

(1) ID	(2) R.A.	(3) Dec.	(4) i (mag ^a)	(5) L	(6) Period ^b (d)	(7) χ^2	(8) Amp (mag)	(9) T_0^c	(10) Type ^d	(11) Note ^e
AST06454	10:51:06.13	-62:49:23.1	12.74	0.76	0.04	...	VAR	...
AST06485	10:51:08.81	-62:53:09.8	13.74	0.90	0.05	...	VAR	...
AST06551	10:51:04.87	-60:45:58.9	13.35	1.15	3.140070915 (583)	0.51	0.08	15431.992237	MP	...
AST06935	10:51:07.08	-60:49:13.1	14.87	2.01	0.404375076 (6)	2.01	0.21	15428.370110	EW-OC	[A,O]
AST06992	10:51:13.05	-62:56:21.9	14.72	2.24	2.859702110 (113)	0.63	0.30	15428.544971	EA	...
AST07161	10:51:12.83	-62:18:16.1	13.98	0.79	0.11	...	VAR	...
AST07651	10:51:12.23	-61:32:00.2	12.74	1.56	0.09	...	VAR	...
AST07839	10:51:14.15	-61:45:24.3	13.20	1.95	0.13	...	VAR	[G]
AST07857	10:51:12.31	-60:54:20.0	12.74	0.89	0.05	...	VAR	...
AST07949	10:51:16.12	-60:44:17.0	15.45	1.57	1.600357056 (64)	0.64	0.36	15429.700244	EA	...
AST08137	10:51:15.13	-60:39:12.6	12.55	0.88	0.05	...	VAR	...
AST08233	10:51:17.71	-60:48:20.5	14.59	0.70	1.310830474 (126)	0.65	0.10	...	MP	...
AST08359	10:51:20.06	-61:59:51.8	14.99	1.41	0.983328998 (63)	1.05	0.10	15428.013721	PER	...
AST08666	10:51:15.25	-60:32:08.2	12.00	10.69	0.398373961 (1)	0.57	0.54	15427.925830	EW	[A,G]
AST08720	10:51:18.04	-60:14:34.2	13.55	1.70	0.629107833 (12)	0.30	0.14	15456.153838	EA	...
AST08781	10:51:23.30	-62:17:45.0	13.46	0.80	0.260562032 (9)	1.07	0.05	15428.100244	DS	...
AST08972	10:51:22.87	-62:13:03.1	12.35	1.06	0.08	...	VAR	...
AST09228	10:51:27.85	-62:01:17.4	15.55	2.31	7.822863579 (967)	0.48	0.41	15428.225586	EA	...
AST09260	10:51:27.26	-61:59:37.4	15.05	2.80	0.603488028 (7)	9.40	0.45	15428.265674	EA	...
AST09282	10:51:23.78	-60:11:49.4	14.07	3.65	2.139209986 (318)	0.50	0.14	15457.765166	PER	...
AST09688	10:51:28.20	-60:34:46.6	15.82	0.77	0.285608947 (7)	1.90	0.17	15427.964893	EA PER	...
AST09763	10:51:24.25	-60:50:36.4	13.86	0.91	0.544745624 (19)	0.75	0.07	15427.966846	EW PER	...
AST10084	10:51:34.84	-62:55:42.6	13.26	2.77	1.228544593 (29)	0.82	0.18	15428.983448	EA	...
AST10364	10:51:39.63	-62:50:31.8	14.41	1.25	0.288527936 (6)	0.70	0.08	15427.904867	EW PER	...
AST10372	10:51:31.04	-60:09:45.6	13.60	0.76	0.04	...	VAR	[G]
AST10395	10:51:35.03	-61:52:57.9	13.59	1.31	0.08	...	VAR	...
AST10442	10:51:32.50	-60:06:42.0	14.64	1.22	0.845150113 (19)	0.54	0.10	15455.538945	MP	...
AST10684	10:51:39.22	-62:04:33.3	15.49	3.08	0.416190863 (5)	0.70	0.33	15428.288135	EW-OC	...
AST11314	10:51:45.40	-62:14:48.0	14.83	0.80	0.782273173 (65)	1.32	0.08	...	MP	...
AST11322	10:51:44.78	-61:59:01.2	15.76	1.25	0.082026005 (1)	0.49	0.22	15428.077198	DS	...
AST11515	10:51:45.30	-61:46:13.0	14.93	6.71	0.367223918 (1)	0.66	0.76	15427.991260	EW	[G]
AST11525	10:51:43.51	-61:02:20.5	15.62	2.55	0.341762990 (3)	0.76	0.61	15428.279867	EW-OC	[A,O,G]
AST11717	10:51:41.96	-61:16:05.2	12.50	1.51	0.13	...	VAR	...
AST11766	10:51:45.65	-61:16:44.8	15.65	0.72	0.529805183 (33)	0.54	0.12	15428.673421	EW PER	...
AST12171	10:51:52.18	-62:53:59.4	13.53	0.97	0.06	...	VAR	...
AST12284	10:51:47.20	-60:27:14.2	15.42	0.94	1.371219635 (43)	0.57	0.30	15456.192901	EA	...
AST12297	10:51:45.13	-60:24:00.8	14.85	0.85	3.703156710 (1783)	0.37	0.08	15459.456573	PER	...
AST12412	10:51:46.90	-60:15:51.3	15.03	1.95	3.401479006 (483)	0.72	0.25	15457.275909	MP	...
AST12477	10:51:49.45	-62:14:25.1	13.72	3.09	3.274060965 (47)	0.69	1.33	15429.622119	EA	...
AST12622	10:51:50.77	-61:40:00.9	14.10	0.87	1.318220377 (130)	0.53	0.08	15429.218799	PER	...
AST12715	10:51:51.20	-60:57:26.3	14.96	1.67	1.026523948 (41)	0.43	0.25	15428.869190	EW-OC	[A,O]
AST13126	10:51:50.85	-61:36:47.7	12.53	1.62	0.08	...	VAR	...
AST13156	10:51:52.66	-60:42:23.8	15.82	0.93	0.414962053 (12)	1.35	0.25	15428.103109	EW-OC	...
AST13387	10:51:54.10	-61:28:02.2	11.93	4.39	4.069720268 (206)	0.18	0.43	...	DCEP	[A,G]
AST13431	10:51:58.32	-61:27:01.5	15.45	0.67	0.17	...	VAR	[A]
AST13448	10:52:02.41	-62:11:40.1	15.16	1.98	2.042309999 (54)	0.58	0.60	15430.961963	EA	...
AST13451	10:51:57.81	-61:07:09.2	14.33	0.78	1.192824006 (61)	0.45	0.12	15429.060596	EA PER	[A,O]
AST14392	10:52:08.26	-62:06:44.3	14.32	1.42	0.525962174 (13)	1.18	0.12	15428.502979	EW PER	...
AST14578	10:52:05.33	-61:20:31.6	13.19	1.98	1.977267146 (34)	0.51	0.27	15429.874724	EA	[A,O,G]
AST14741	10:52:10.46	-62:03:19.1	13.96	0.87	0.04	...	VAR	...
AST15267	10:52:12.44	-61:20:12.3	14.64	1.14	2.827423811 (429)	0.43	0.10	15430.448291	EW PER	...
AST15280	10:52:10.47	-60:35:41.6	15.70	1.47	1.597659945 (36)	0.83	0.62	15428.646533	EA	[G]
AST15337	10:52:10.16	-60:40:43.1	14.27	1.52	0.09	...	VAR	...
AST15400	10:52:07.35	-60:34:23.1	12.47	2.09	0.11	...	VAR	...
AST15457	10:52:07.66	-60:38:29.2	12.72	1.02	0.05	...	VAR	...
AST15912	10:52:20.45	-62:06:50.1	14.29	3.89	0.830626786 (13)	0.41	0.27	15428.783252	EW-OC	...
AST16017	10:52:17.93	-61:20:10.3	13.77	0.70	0.07	...	VAR	[G]
AST16189	10:52:18.24	-62:16:59.9	13.42	1.93	0.12	...	VAR	...
AST16271	10:52:12.37	-60:33:46.0	12.33	2.24	3.441099882 (90)	0.68	0.26	15429.156299	EA	...
AST16336	10:52:09.47	-61:25:46.2	12.09	0.95	0.08	...	VAR	[G]
AST16337	10:52:18.49	-60:47:01.2	14.21	0.70	3.435531855 (497)	6.29	0.13	...	PER	...
AST16396	10:52:12.11	-60:32:20.4	13.39	1.39	0.09	...	VAR	...
AST16539	10:52:22.98	-61:32:08.7	13.81	7.16	7.395895958 (446)	0.31	0.62	15439.385742	EB	[G]
AST16578	10:52:15.25	-60:24:13.0	12.05	1.38	0.607649922 (20)	0.17	0.10	15456.536651	EW	[G]
AST16587	10:52:23.55	-61:57:47.6	13.52	1.05	1.588346481 (282)	0.45	0.05	15428.842823	PER	...
AST16670	10:52:15.97	-60:23:47.8	12.75	5.18	0.28	...	VAR	[G]
AST16693	10:52:21.08	-60:33:35.4	15.91	1.08	1.242375016 (59)	0.51	0.65	15429.258838	EA	[G]
AST16917	10:52:19.39	-60:49:07.0	13.31	0.86	0.08	...	VAR	...
AST16928	10:52:29.48	-62:08:26.8	14.32	0.77	0.828264415 (56)	0.43	0.07	15428.339893	EW PER	...
AST16981	10:52:24.56	-60:57:17.6	15.00	1.53	0.447291791 (12)	0.61	0.19	15428.528890	EW-OC	...
AST17108	10:52:31.84	-62:21:48.7	15.19	3.23	0.882196426 (20)	1.12	0.35	15428.790088	EW-OC	...
AST17511	10:52:28.94	-61:04:35.6	15.05	1.03	0.443277836 (14)	0.79	0.10	15428.052783	EW PER	...
AST17592	10:52:29.42	-61:14:58.9	13.42	1.11	0.07	...	VAR	...

TABLE 2 — *Continued*

(1) ID	(2) R.A.	(3) Dec.	(4) i (mag ^a)	(5) L	(6) Period ^b (d)	(7) χ^2	(8) Amp (mag)	(9) T_0^c	(10) Type ^d	(11) Note ^e
AST17775	10:52:33.12	-61:29:05.4	15.45	1.61	2.391628981 (217)	0.74	0.31	15430.316455	DCEP	[A,O]
AST17892	10:52:37.23	-62:05:37.3	15.38	1.97	3.269760847 (490)	0.53	0.25	15430.398031	EW-OC PER	...
AST17934	10:52:31.44	-60:51:40.5	14.35	1.48	0.14	...	VAR	...
AST17938	10:52:32.07	-60:56:32.3	15.99	1.41	1.413506150 (51)	0.62	0.44	15429.412158	EA	[A,O]
AST17970	10:52:24.54	-60:34:38.2	12.09	0.91	0.07	...	VAR	[G]
AST18237	10:52:30.09	-60:07:42.7	15.58	1.75	0.854213774 (14)	1.08	0.74	15456.284698	EA	...
AST18432	10:52:42.11	-62:15:18.1	15.60	0.90	1.822781205 (44)	0.57	0.27	15428.615283	EA	...
AST18438	10:52:32.39	-60:25:05.9	14.57	0.71	2.720453978 (122)	0.76	0.16	15456.515166	EA	...
AST18697	10:52:33.02	-60:29:20.1	13.24	0.77	0.05	...	VAR	...
AST18843	10:52:34.49	-60:35:45.9	12.39	0.84	0.05	...	VAR	...
AST18900	10:52:38.80	-60:51:02.1	14.87	1.70	0.390786111 (10)	0.60	0.12	15428.069385	EW-OC PER	[A,O]
AST19345	10:52:45.70	-61:43:51.3	14.27	1.07	0.08	...	VAR	...
AST19397	10:52:46.50	-61:56:32.8	12.94	2.28	1.487738967 (40)	2.12	0.17	15429.200244	EA EB	[G]
AST19490	10:52:40.15	-60:17:49.6	13.74	1.19	0.07	...	VAR	...
AST19571	10:52:50.42	-61:55:57.3	15.52	3.60	0.523991883 (7)	0.69	0.51	15428.272054	EW	[A,O,G]
AST19702	10:52:40.54	-60:14:30.6	13.11	0.72	0.06	...	VAR	...
AST19762	10:52:43.98	-60:40:21.9	14.27	0.71	0.07	...	VAR	...
AST19802	10:52:52.71	-62:09:08.3	15.12	1.73	1.435382485 (35)	1.34	0.38	15428.928760	EA	...
AST20003	10:52:48.50	-61:20:33.1	13.02	1.37	0.12	...	VAR	[G]
AST20105	10:52:56.09	-62:22:09.6	14.96	1.52	2.558847904 (102)	0.69	0.37	15429.147510	EA	...
AST20541	10:52:43.12	-60:08:53.2	12.53	0.77	0.05	...	VAR	...
AST20657	10:52:51.86	-61:21:25.8	13.44	5.67	0.547526121 (6)	0.33	0.21	15428.025440	EW	[A,O,G]
AST20751	10:52:55.61	-61:20:22.8	14.80	0.98	1.859558702 (140)	0.72	0.19	15429.148487	EA	[A,O]
AST21008	10:52:48.78	-60:39:16.4	12.57	6.76	0.40	...	VAR	[G]
AST21541	10:52:56.62	-60:24:24.0	15.59	3.48	0.425307095 (5)	0.52	0.48	15455.772979	EW	...
AST21898	10:53:03.31	-61:38:22.1	13.21	2.84	1.577608943 (25)	0.32	0.33	15429.568408	EA EB	[A,O,G]
AST21960	10:53:00.44	-61:31:28.6	12.94	0.70	1.152198195 (131)	0.45	0.04	15428.828174	GD	...
AST22118	10:53:01.35	-61:07:28.0	12.06	0.80	0.07	...	VAR	[G]
AST22460	10:53:09.66	-62:08:12.9	13.21	1.06	0.07	...	VAR	...
AST22946	10:53:09.45	-60:56:28.7	14.66	1.98	0.656189680 (23)	0.54	0.14	15428.748096	EW	...
AST22962	10:53:10.61	-61:11:00.5	15.10	1.38	0.282831937 (4)	4.26	0.15	15428.128955	EW PER	[A,O]
AST23276	10:53:08.51	-60:23:33.8	14.34	0.74	1.510576248 (155)	0.63	0.05	15456.063995	MP?	...
AST23445	10:53:08.01	-60:08:52.9	14.34	4.33	3.660130024 (494)	0.39	0.31	...	DCEP	[G]
AST23515	10:53:16.79	-61:14:36.0	15.20	1.04	3.664343834 (111)	0.86	0.28	15429.375049	EA	[A,O]
AST23549	10:53:17.02	-62:11:11.9	12.43	1.04	0.05	...	VAR	[G]
AST23732	10:53:26.97	-62:50:34.0	13.71	7.34	1.148756146 (8)	0.73	0.47	15428.734424	EW	[G]
AST24162	10:53:20.84	-61:12:34.7	14.52	1.35	0.20	...	VAR	[G]
AST24293	10:53:15.80	-60:06:10.9	15.22	1.02	1.696804285 (56)	0.53	0.33	15456.459502	EA	...
AST24378	10:53:18.86	-60:40:31.6	13.78	4.50	1.162574887 (20)	2.29	0.34	15429.216846	EB PER	...
AST24383	10:53:25.13	-61:50:57.6	13.98	0.94	0.08	...	VAR	...
AST24483	10:53:20.10	-60:51:15.7	14.22	5.41	0.32	...	VAR	[G]
AST24488	10:53:22.64	-61:09:59.6	13.62	1.27	1.223636627 (84)	0.61	0.05	15428.988330	EW PER	...
AST24519	10:53:24.91	-61:36:12.9	13.62	1.38	1.013308048 (17)	0.43	0.31	15428.983448	EA	...
AST24595	10:53:27.96	-61:47:05.0	15.02	1.15	1.151387572 (64)	0.50	0.15	15428.665088	EA	[A,O]
AST24761	10:53:31.41	-62:03:36.0	14.65	3.78	0.960982978 (19)	0.42	0.49	15428.367237	EB-OC	[G]
AST24936	10:53:34.41	-62:19:58.8	14.94	1.03	0.12	...	VAR	[G]
AST25082	10:53:20.23	-60:29:51.8	12.43	0.93	0.10	...	VAR	[G]
AST25627	10:53:29.57	-60:38:48.5	15.98	0.96	0.371532083 (5)	3.05	0.60	15428.250049	EW	...
AST25633	10:53:33.00	-61:29:16.1	13.91	2.81	3.507858992 (96)	0.51	0.51	...	EA	[G]
AST25740	10:53:36.00	-61:32:53.6	15.71	0.84	1.584113002 (151)	0.56	0.19	15428.189502	EA	[A]
AST25746	10:53:32.06	-61:26:53.4	13.29	1.29	0.08	...	VAR	...
AST25809	10:53:34.00	-61:37:04.7	13.44	1.00	1.191421747 (100)	0.95	0.05	15428.616260	PER	...
AST26037	10:53:33.61	-61:03:36.8	13.69	4.42	0.25	...	VAR	[G]
AST26542	10:53:35.79	-61:24:16.4	12.56	1.61	2.834712982 (92)	1.03	0.29	15429.387744	EA	[G]
AST26602	10:53:41.52	-61:36:54.1	14.25	0.94	2.780464172 (57)	1.65	0.16	15431.603750	EA	[A,G]
AST26987	10:53:45.46	-61:45:38.5	13.15	1.10	0.07	...	VAR	...
AST27264	10:53:35.65	-60:21:14.2	12.95	2.31	0.14	...	VAR	[G]
AST27396	10:53:45.46	-61:15:34.9	13.81	8.67	0.417315871 (2)	0.54	0.44	15427.911182	EW-OC	[A,O,G]
AST27409	10:53:50.87	-62:12:28.5	13.72	1.16	2.180987358 (139)	0.42	0.17	15428.778369	EA	...
AST27423	10:53:46.54	-61:44:27.0	12.91	1.87	2.292398691 (384)	0.50	0.07	...	PER	...
AST27446	10:53:40.56	-60:41:23.0	13.38	0.94	0.06	...	VAR	[G]
AST27616	10:53:51.09	-61:43:00.7	15.10	3.42	0.384974092 (3)	0.44	0.37	15427.903369	EW	[A,O,G]
AST27693	10:53:43.12	-60:44:55.0	13.68	0.99	0.804831743 (17)	0.43	0.14	15428.485401	EA	...
AST28128	10:53:58.08	-62:15:55.9	13.95	13.00	1.843686104 (27)	5.13	0.55	15429.411182	DCEP	...
AST28261	10:53:59.01	-62:21:33.5	13.20	1.16	0.12	...	VAR	...
AST28305	10:54:02.19	-62:29:22.3	14.55	3.22	0.344083905 (3)	0.51	0.23	15428.029346	EW-OC	...
AST28312	10:53:52.06	-61:11:21.8	14.32	0.91	0.07	...	VAR	...
AST28392	10:54:00.77	-62:07:23.5	16.09	1.90	0.363243043 (5)	0.53	0.69	15428.054737	EW	...
AST28525	10:53:53.89	-61:02:43.9	16.05	1.47	0.497086167 (14)	1.49	0.38	15428.055713	PER	...
AST28541	10:54:07.05	-62:52:47.8	14.61	4.99	0.441091061 (3)	0.85	0.33	15428.212940	EW	...
AST28591	10:53:57.54	-61:40:28.7	13.86	2.46	3.233769655 (87)	0.63	0.31	15430.993213	EA	[G]
AST28592	10:53:55.54	-61:28:13.9	13.53	1.22	1.850862265 (29)	0.34	0.37	15429.826221	EA	[G]
AST28694	10:53:47.52	-60:33:12.8	11.95	1.63	0.14	...	VAR	[G]

TABLE 2 — *Continued*

(1) ID	(2) R.A.	(3) Dec.	(4) i (mag ^a)	(5) L	(6) Period ^b (d)	(7) χ^2	(8) Amp (mag)	(9) T_0^c	(10) Type ^d	(11) Note ^e
AST28842	10:53:49.56	-60:10:28.5	15.23	0.72	0.832642198 (92)	0.54	0.08	15456.691924	MP	...
AST28998	10:54:03.15	-62:07:32.1	14.17	1.35	0.560002744 (23)	0.35	0.09	15428.401416	EB	...
AST29379	10:53:51.00	-60:15:27.4	13.24	0.99	0.07	...	VAR	[G]
AST29542	10:54:01.83	-61:09:28.0	14.90	2.00	1.456911564 (26)	0.58	0.51	15429.487354	EA	[A,O]
AST30089	10:54:03.02	-60:45:49.0	15.08	0.96	0.674265802 (34)	1.17	0.10	...	MP	...
AST30454	10:54:03.07	-60:19:17.6	15.87	1.48	0.977033973 (30)	0.87	0.37	15456.120635	EA EB	...
AST30846	10:54:05.48	-60:37:27.7	12.15	1.36	0.08	...	VAR	[G]
AST30972	10:54:20.12	-62:26:53.6	12.87	0.74	0.07	...	VAR	...
AST31346	10:54:13.57	-61:08:30.8	13.41	0.89	0.07	...	VAR	...
AST31414	10:54:10.60	-60:30:23.3	15.36	1.16	0.897397995 (19)	0.54	0.44	15428.017627	EA EB	...
AST31492	10:54:18.96	-61:35:09.7	16.23	0.83	0.376334101 (17)	1.26	0.27	15427.947836	MP	[A,O]
AST31705	10:54:21.06	-61:28:57.6	15.32	2.69	1.405745387 (57)	0.98	0.39	15428.174854	EW	[A,O]
AST31708	10:54:13.36	-60:34:53.1	15.69	1.44	0.580020070 (16)	1.18	0.51	15428.633122	RRAB	...
AST32315	10:54:32.08	-62:17:49.1	14.46	0.74	1.061147928 (32)	0.48	0.13	15428.913135	EA	...
AST32456	10:54:20.75	-60:55:33.7	14.70	3.63	0.279452026 (3)	1.03	0.31	15428.039112	RRC	...
AST32504	10:54:18.70	-60:32:34.3	13.77	0.87	1.175762773 (111)	0.40	0.05	15428.931690	EB PER	...
AST32604	10:54:17.71	-60:23:02.7	14.27	1.34	3.658822775 (300)	0.58	0.17	15459.938018	MP	...
AST33265	10:54:26.87	-61:20:49.6	11.29	1.80	4.705473900 (665)	0.13	0.41	15431.933187	DCEP	[A,G]
AST33315	10:54:39.04	-62:12:34.9	14.55	2.81	0.345232904 (8)	1.27	0.18	15428.012289	RRC EW	...
AST33563	10:54:40.63	-62:05:47.9	14.53	1.32	3.494258881 (144)	0.50	0.32	15430.169971	EA	...
AST34380	10:54:48.08	-62:15:51.1	15.77	0.93	1.506839395 (50)	0.56	0.65	15429.258838	EA	...
AST34755	10:54:35.99	-60:30:13.5	14.87	0.97	0.756472111 (14)	0.93	0.40	15428.877002	EA	...
AST35419	10:54:47.89	-61:22:51.1	14.14	1.93	2.303624392 (343)	0.88	0.10	15430.683643	PER	...
AST35518	10:54:47.31	-61:45:04.2	12.85	1.68	1.670595169 (194)	0.36	0.08	15429.008838	PER	...
AST35527	10:54:41.80	-60:40:12.2	13.68	1.02	7.527365208 (1026)	-NaN	0.07	15429.567953	PER	...
AST35554	10:54:45.18	-60:53:14.7	14.97	0.70	2.548235416 (104)	0.91	0.26	15430.415088	EA	[A,O]
AST35618	10:54:42.65	-60:46:46.6	13.76	0.74	0.06	...	VAR	[G]
AST36262	10:54:49.01	-60:40:40.6	15.96	1.95	0.831375599 (16)	0.68	0.81	15428.657276	EB	[G]
AST36515	10:55:04.42	-62:19:20.0	13.82	0.74	0.05	...	VAR	...
AST36836	10:55:01.32	-61:42:46.3	14.91	1.36	0.599171996 (12)	1.63	0.35	15428.388072	EW-OC	...
AST36837	10:55:00.13	-61:40:00.3	13.12	1.74	1.911146045 (129)	0.54	0.11	15429.260791	EW	...
AST36995	10:55:08.68	-62:12:47.8	15.23	1.20	4.800000191 (148)	3.90	0.72	15454.918018	EA	...
AST37278	10:54:51.51	-60:15:55.8	13.86	0.81	1.449908495 (188)	0.27	0.04	15457.181182	EW PER	...
AST37300	10:55:05.30	-61:39:29.4	14.34	0.98	0.11	...	VAR	...
AST37460	10:55:02.95	-61:16:31.0	14.25	1.21	0.13	...	VAR	...
AST37489	10:55:08.64	-61:43:59.2	15.81	0.85	0.735394716 (30)	4.13	0.44	15428.645557	EB	[A,O]
AST37704	10:55:14.40	-62:36:05.8	13.35	0.97	0.10	...	VAR	[G]
AST37735	10:55:02.52	-61:08:57.2	13.18	1.14	0.08	...	VAR	...
AST37813	10:55:13.07	-62:06:33.8	13.61	0.67	0.08	...	VAR	...
AST37940	10:55:10.04	-61:35:08.5	15.44	1.20	1.760604978 (53)	0.47	0.68	15429.831104	EA	[A,O,G]
AST38108	10:55:07.42	-61:23:45.5	14.93	0.79	0.790589273 (43)	2.12	0.19	...	RRAB	...
AST38214	10:55:18.37	-62:26:19.1	13.65	1.38	0.11	...	VAR	[G]
AST38428	10:55:11.97	-61:42:24.4	11.84	1.09	0.13	...	VAR	[G]
AST38503	10:55:06.81	-60:48:49.5	15.18	3.54	0.866045535 (20)	0.74	0.40	15428.149007	EW	...
AST38528	10:55:21.71	-62:25:06.1	14.59	0.76	0.07	...	VAR	...
AST38531	10:55:14.23	-61:37:21.9	15.37	0.76	3.240096092 (101)	2.50	0.62	15429.458057	EA	[A,O]
AST38733	10:55:28.68	-62:50:28.4	15.04	3.16	0.429434806 (5)	0.44	0.25	15428.062549	EW	...
AST38989	10:55:12.18	-60:58:19.3	15.51	1.29	1.579001188 (35)	0.76	0.56	15428.886768	EA	[A,O]
AST39051	10:55:16.45	-61:36:23.0	12.98	0.70	0.04	...	VAR	[G]
AST39275	10:55:05.64	-60:06:58.4	15.37	0.81	0.10	...	VAR	...
AST39579	10:55:12.53	-60:34:10.4	15.53	2.56	0.710536838 (16)	0.92	0.33	15428.539112	EW	[A,O]
AST39766	10:55:07.66	-60:04:37.3	13.66	3.14	3.126559973 (76)	0.32	0.80	15459.139190	EA	[G]
AST39901	10:55:25.98	-61:41:08.7	15.68	1.07	0.597742140 (24)	1.24	0.20	...	MP	[A,O]
AST39979	10:55:09.10	-60:32:51.8	11.08	1.08	5.495259762 (1338)	0.06	0.39	...	DCEP	[A,G]
AST40037	10:55:29.18	-62:04:08.2	13.84	5.63	0.311896056 (2)	1.80	0.29	15428.130908	EW-OC	...
AST40137	10:55:31.23	-62:11:43.0	13.36	4.52	0.564102173 (5)	0.31	0.27	15428.466846	EB	[G]
AST40361	10:55:23.18	-61:08:01.6	15.63	0.75	0.19	...	VAR	...
AST40531	10:55:18.29	-60:25:52.5	15.85	0.87	1.720689893 (58)	0.53	0.39	15456.416534	EA	...
AST40536	10:55:21.58	-60:54:55.6	14.03	1.29	3.906109333 (82)	1.53	0.25	15429.293018	EA	[A,O,G]
AST40551	10:55:17.20	-60:34:01.3	12.92	4.25	3.180012941 (289)	0.61	0.19	15430.945362	PER	...
AST40565	10:55:23.95	-61:15:58.8	13.13	0.97	0.254520088 (5)	0.71	0.04	15427.975635	EW	...
AST40655	10:55:32.03	-61:49:49.5	14.64	1.02	0.826864839 (21)	0.87	0.17	15428.421924	EA	[A,O]
AST40671	10:55:21.73	-60:50:31.5	13.74	3.44	3.720889091 (122)	2.45	0.32	15431.042041	EA	[A,O,G]
AST40766	10:55:23.08	-60:50:51.4	14.23	3.30	1.205307245 (22)	0.41	0.35	15428.075244	EB	[A,O,G]
AST40904	10:55:24.62	-60:48:42.4	14.55	2.34	1.436740637 (27)	10.67	0.44	15430.209033	EA	[A,O]
AST40957	10:55:12.26	-60:09:30.3	12.05	6.60	0.62	...	VAR	[G]
AST40966	10:55:36.09	-61:58:54.4	14.83	0.82	0.369984895 (8)	1.24	0.10	15428.098633	EW DS	...
AST41209	10:55:23.77	-60:34:06.9	14.37	0.93	0.11	...	VAR	[G]
AST41484	10:55:39.68	-62:18:07.9	11.74	1.23	0.16	...	VAR	[G]
AST41594	10:55:41.59	-61:52:24.9	15.47	2.48	0.980476022 (38)	1.79	0.28	15428.038135	EW	[A,O]
AST41650	10:55:41.79	-62:23:58.2	12.46	1.05	0.10	...	VAR	[G]
AST41745	10:55:24.49	-60:21:29.5	14.88	1.01	1.285867810 (72)	0.80	0.26	15457.657745	EA	[A,O]
AST41973	10:55:42.14	-61:42:45.2	14.93	0.68	0.244695961 (6)	0.87	0.07	15428.032796	EW DS	...

TABLE 2 — *Continued*

(1) ID	(2) R.A.	(3) Dec.	(4) i (mag ^a)	(5) L	(6) Period ^b (d)	(7) χ^2	(8) Amp (mag)	(9) T_0^c	(10) Type ^d	(11) Note ^e
AST42266	10:55:39.27	-61:26:18.2	12.38	1.57	0.10	...	VAR	...
AST42287	10:55:36.50	-60:56:50.2	15.07	1.00	3.011338949 (174)	0.55	0.21	15428.702198	EA	[A,O]
AST42467	10:55:33.33	-60:36:53.8	14.54	1.39	0.13	...	VAR	...
AST42471	10:55:45.35	-61:42:00.0	14.69	0.68	1.380798340 (240)	0.36	0.06	15429.068018	PER	...
AST42633	10:55:36.28	-60:39:30.5	15.67	1.12	0.529599667 (19)	0.96	0.18	15428.054281	EW	[A,O]
AST42854	10:55:45.13	-61:40:04.9	12.94	2.17	0.11	...	VAR	[G]
AST42869	10:55:45.83	-61:29:11.4	14.57	1.84	5.210867882 (190)	0.58	0.39	15434.615283	EA	[A,O]
AST43064	10:55:34.27	-60:25:44.2	12.25	1.76	3.294270754 (813)	0.16	0.08	15459.939971	PER	[A]
AST43091	10:55:52.82	-62:18:28.3	12.97	1.57	0.07	...	VAR	...
AST43350	10:55:49.11	-61:19:56.7	15.44	2.35	0.348057121 (5)	0.70	0.29	15428.060596	EW	[A,O]
AST43409	10:55:34.25	-60:04:59.0	13.46	2.05	0.15	...	VAR	[G]
AST43421	10:55:36.80	-60:13:03.9	14.55	1.09	2.331650019 (99)	1.12	0.26	15457.692901	EA	[A,O]
AST43483	10:55:55.39	-61:53:26.8	14.17	1.21	0.09	...	VAR	...
AST43594	10:55:41.33	-60:26:24.2	14.78	4.59	1.319027424 (36)	1.39	0.34	15456.387237	EW	[A,O]
AST43846	10:56:05.91	-62:29:46.4	14.31	1.53	0.16	...	VAR	[G]
AST44047	10:55:54.02	-61:48:38.3	15.16	1.39	0.18	...	VAR	...
AST44142	10:56:00.05	-61:53:36.9	14.77	5.21	3.456959963 (88)	0.45	0.74	15429.667041	EA	[A,O,G]
AST44299	10:55:46.51	-60:43:14.0	12.99	0.94	0.05	...	VAR	...
AST44490	10:56:06.39	-62:10:40.4	14.28	0.74	0.06	...	VAR	...
AST44663	10:55:53.76	-60:51:03.7	14.87	1.22	0.367153913 (9)	1.54	0.10	15428.104541	EW PER	...
AST45236	10:55:57.07	-60:47:19.7	15.58	0.87	0.470419914 (20)	0.92	0.15	15428.452198	EW-OC PER	[A,O]
AST45483	10:56:00.72	-61:00:16.0	14.88	1.93	1.544415832 (47)	0.74	0.29	15429.040088	EA	[A,O]
AST45682	10:55:54.71	-60:31:55.1	11.98	1.48	0.559423745 (19)	1.63	0.11	15428.278369	MP	[G]
AST46247	10:56:07.39	-60:57:59.7	15.52	2.12	0.373133093 (7)	0.49	0.24	15428.302783	EW	[A,O]
AST46248	10:55:58.69	-60:08:55.0	15.75	1.08	1.423607945 (32)	0.45	0.68	15455.928252	EA	...
AST46259	10:56:12.29	-61:39:04.8	12.46	2.48	0.20	...	VAR	...
AST46538	10:56:04.08	-60:41:49.7	12.50	5.74	0.332560122 (2)	0.56	0.28	15428.296924	EW-OC	[G]
AST46624	10:56:07.27	-60:54:07.9	12.83	0.73	0.05	...	VAR	[G]
AST46738	10:56:22.40	-61:59:35.1	13.36	0.79	0.06	...	VAR	[G]
AST46831	10:56:23.01	-62:08:52.8	12.40	0.70	0.05	...	VAR	...
AST46971	10:56:02.84	-60:14:08.6	12.77	1.06	4.698013783 (183)	0.39	0.17	15459.567901	EA	[G]
AST47752	10:56:24.33	-61:40:25.7	13.17	0.78	0.754773319 (66)	0.44	0.04	15428.530323	PER	...
AST47810	10:56:13.06	-60:36:54.7	15.76	1.62	0.232284963 (4)	5.00	0.27	15428.055713	MP	...
AST48113	10:56:27.76	-61:38:18.5	14.71	0.87	0.347427934 (12)	1.06	0.06	15428.090869	EW DS	...
AST48273	10:56:27.91	-61:36:42.6	15.22	0.94	1.041998029 (51)	1.18	0.17	15428.113330	EA PER	...
AST48567	10:56:16.57	-60:36:14.5	15.04	0.71	0.472171098 (21)	1.12	0.08	...	MP	...
AST48664	10:56:37.53	-62:18:55.8	12.32	1.24	1.096216321 (48)	0.25	0.09	15429.486377	EW	[G]
AST49035	10:56:27.03	-60:56:12.7	14.19	1.62	0.15	...	VAR	[A,O,G]
AST49082	10:56:26.29	-60:51:33.4	15.24	2.61	0.632324636 (11)	2.11	0.40	15428.699268	EW	...
AST49241	10:56:28.18	-61:12:02.4	12.58	0.69	1.638723373 (281)	0.32	0.04	15428.926807	PER	...
AST49631	10:56:40.04	-61:53:57.9	13.09	1.86	0.15	...	VAR	...
AST50202	10:56:47.48	-61:56:02.8	14.24	1.89	0.130455017 (1)	0.49	0.12	15427.906299	DS	...
AST50267	10:56:26.13	-60:12:32.8	15.37	0.92	0.582240939 (17)	0.59	0.23	15455.982940	EA	[A,O]
AST50549	10:56:30.72	-60:31:50.2	13.88	0.91	1.230798006 (22)	0.40	0.48	15456.821183	EA	[A,O]
AST50581	10:56:26.85	-60:17:04.9	12.58	0.91	0.08	...	VAR	[G]
AST50984	10:56:46.78	-61:26:04.2	14.77	1.13	0.10	...	VAR	...
AST51624	10:56:35.38	-60:12:39.1	13.37	3.66	1.533192635 (54)	0.31	0.18	15457.358916	EB	[A,O,G]
AST51948	10:57:08.68	-62:35:21.8	13.58	1.20	0.08	...	VAR	...
AST52507	10:56:46.21	-60:42:26.1	14.18	1.00	0.09	...	VAR	...
AST52618	10:57:00.15	-61:35:04.4	14.20	0.75	0.333141983 (12)	0.93	0.05	15455.707549	EW PER	...
AST53068	10:57:11.92	-62:20:18.8	12.42	0.70	0.04	...	VAR	...
AST53255	10:56:57.55	-61:09:04.3	13.16	1.88	2.278520823 (216)	0.56	0.09	15457.303252	PER	...
AST53328	10:57:10.14	-62:11:12.1	13.43	1.69	0.143530995 (2)	4.00	0.07	15455.716338	DS	...
AST53334	10:56:45.63	-60:04:32.0	14.02	1.07	0.385251939 (10)	0.59	0.09	15455.992705	EW	...
AST53357	10:56:46.85	-60:14:42.1	14.90	5.02	0.356884986 (1)	1.24	0.86	15455.919463	EW	[A,O,G]
AST53582	10:57:18.79	-62:24:23.9	15.08	1.70	3.934043884 (765)	0.64	0.18	15456.464385	PER	...
AST53821	10:56:56.39	-60:40:13.2	13.64	0.92	0.05	...	VAR	[G]
AST53841	10:57:19.40	-62:34:18.6	11.94	0.93	0.09	...	VAR	[G]
AST54338	10:57:04.00	-60:53:37.9	15.75	1.13	0.386257917 (11)	1.13	0.18	15455.932159	EW-OC	[A,O]
AST54349	10:56:57.83	-60:25:06.5	14.81	2.16	0.287913978 (1)	2.87	0.52	15455.644073	EW-OC	[A,O]
AST54537	10:57:06.53	-61:01:12.1	13.54	6.16	2.962728024 (21)	2.09	1.32	15456.965362	EA	[A,O,G]
AST54552	10:57:21.33	-62:10:02.0	13.77	0.68	0.05	...	VAR	...
AST54590	10:57:15.01	-61:34:03.3	14.67	5.44	0.926824987 (5)	0.91	1.23	15456.758330	EA EB	[A,O,G]
AST54604	10:57:19.23	-61:58:44.1	14.16	1.00	2.200000048 (55)	1.13	0.23	15456.295440	EA	...
AST55024	10:57:07.50	-60:47:17.8	15.38	0.85	0.828652203 (26)	0.55	0.20	15456.043487	EA	[A,O]
AST55167	10:57:30.88	-62:31:16.8	13.74	1.21	0.07	...	VAR	[G]
AST55196	10:57:20.34	-61:37:00.3	16.08	1.99	0.441311985 (8)	0.64	0.45	15455.693877	EW	...
AST55253	10:57:10.80	-60:51:21.9	15.58	1.30	4.309783936 (869)	0.47	0.22	15457.232940	PER	...
AST55334	10:57:01.04	-60:15:02.9	13.04	2.88	2.966520071 (64)	0.41	0.29	15457.888213	EA	[G]
AST55351	10:57:29.82	-62:18:16.0	13.83	0.73	0.06	...	VAR	...
AST55752	10:57:21.40	-61:43:13.4	13.60	0.83	0.07	...	VAR	...
AST55824	10:57:08.06	-60:24:24.1	15.19	0.81	0.11	...	VAR	...
AST56058	10:57:29.85	-61:52:00.3	14.72	1.37	2.821491003 (194)	0.38	0.51	15459.187041	EA	[A,O,G]

TABLE 2 — *Continued*

(1) ID	(2) R.A.	(3) Dec.	(4) i (mag ^a)	(5) L	(6) Period ^b (d)	(7) χ^2	(8) Amp (mag)	(9) T_0^c	(10) Type ^d	(11) Note ^e
AST56095	10:57:09.66	-60:22:14.3	14.67	1.84	1.975157976 (74)	0.95	0.18	15457.733916	EA PER	...
AST56173	10:57:06.48	-60:11:39.9	14.53	0.95	0.06	...	VAR	...
AST56219	10:57:26.04	-61:32:20.8	14.43	2.03	0.532076061 (12)	0.38	0.16	15456.005401	EW-OC	...
AST56493	10:57:35.02	-62:04:49.7	12.97	2.96	0.22	...	VAR	...
AST56624	10:57:44.81	-62:39:35.3	13.56	4.17	0.709099114 (8)	0.32	0.31	15456.135284	EB	[G]
AST56993	10:57:29.07	-61:39:40.6	12.60	1.11	0.06	...	VAR	[G]
AST57345	10:57:21.60	-60:41:53.2	15.17	0.69	0.08	...	VAR	...
AST57491	10:57:18.96	-60:18:25.3	15.64	2.44	1.887721539 (75)	2.09	0.70	15457.099151	EA	[A,O]
AST57853	10:57:50.95	-62:31:51.1	13.49	1.57	0.15	...	VAR	...
AST57906	10:57:42.52	-61:52:17.0	13.27	1.64	0.480562925 (7)	3.30	0.10	15456.015166	EW PER	...
AST57964	10:57:43.40	-61:50:10.1	15.14	1.14	0.12	...	VAR	...
AST58731	10:57:52.08	-62:01:52.3	15.39	1.28	0.393677950 (10)	1.07	0.17	15455.633330	EW PER	...
AST58825	10:57:25.32	-60:08:47.7	14.69	1.58	1.710039496 (115)	2.35	0.11	...	MP	...
AST58900	10:57:24.27	-60:15:57.7	14.59	0.75	4.699999809 (234)	0.62	0.20	15460.579620	EA	...
AST59186	10:57:52.76	-61:52:01.1	15.26	1.70	1.427323580 (52)	3.83	0.52	15456.567901	EB	[A,O]
AST59410	10:57:56.16	-62:02:08.2	14.96	1.80	0.418405950 (7)	1.73	0.20	15456.181182	EW	...
AST59773	10:57:46.79	-61:12:14.6	15.47	0.99	1.339923859 (54)	0.75	0.24	15455.911651	EA	[A,O]
AST60119	10:57:34.91	-60:21:04.8	13.56	0.72	0.06	...	VAR	[G]
AST60221	10:57:32.80	-60:11:56.5	12.89	1.57	1.650184274 (100)	1.99	0.08	15457.878448	MP	...
AST61020	10:57:44.56	-60:31:22.0	14.87	1.08	1.165158987 (98)	0.42	0.10	15456.215362	EW-OC PER	...
AST61176	10:57:52.28	-60:55:51.4	15.15	3.40	0.381975025 (4)	2.41	0.39	15455.847198	EW	[A,O]
AST61299	10:58:17.11	-62:36:23.9	13.16	1.19	0.07	...	VAR	[G]
AST61303	10:58:06.80	-62:02:39.8	14.39	1.13	0.394757956 (12)	1.49	0.08	15455.618682	DS	...
AST61514	10:57:58.80	-61:45:17.8	11.63	1.29	0.15	...	VAR	[G]
AST61607	10:58:10.07	-61:51:48.0	15.87	1.04	0.928019166 (22)	0.41	0.64	15456.250518	EA	[A,O]
AST61969	10:57:57.41	-60:57:00.3	14.45	1.43	3.344052076 (222)	0.49	0.26	15457.584502	EA	[A,O,G]
AST62031	10:58:11.31	-61:45:33.8	15.05	1.95	0.508938134 (18)	3.47	0.20	15455.904815	PER	...
AST62121	10:58:04.71	-61:22:28.9	14.91	1.59	4.820000172 (166)	0.59	0.53	15460.830596	EA	[A,O,G]
AST62331	10:58:07.53	-61:26:42.9	15.30	1.07	0.624118149 (19)	1.16	0.25	15455.881377	EA	[A,O]
AST62372	10:57:48.81	-60:12:34.3	13.87	2.88	2.180143595 (32)	0.84	0.39	15456.820830	EA	[A,O,G]
AST62577	10:58:31.14	-62:44:37.7	15.44	0.79	0.13	...	VAR	...
AST62838	10:58:02.88	-61:08:57.7	14.98	1.14	1.763568044 (57)	0.92	0.49	15456.709502	EA	[G]
AST62877	10:57:55.65	-60:26:43.1	15.03	3.05	0.700860083 (13)	6.90	0.41	15456.188995	EW-OC PER	[A,O]
AST62975	10:58:23.44	-62:19:59.1	13.75	0.96	0.08	...	VAR	...
AST63063	10:58:06.82	-61:02:15.1	14.66	1.44	3.809439898 (100)	3.02	0.50	...	EA	[A,O]
AST63331	10:57:57.13	-60:11:42.4	15.50	1.02	1.051903009 (23)	0.58	0.38	15456.558135	EA	[A,O]
AST63530	10:58:06.87	-60:56:39.4	14.66	0.82	0.433721989 (13)	0.94	0.08	15455.646026	EW DS	...
AST64031	10:58:08.01	-60:38:30.1	15.38	0.82	0.315470010 (7)	1.85	0.14	15455.787627	EW DS	[A,O]
AST64129	10:58:12.56	-60:54:51.8	13.97	3.38	0.834581017 (20)	0.31	0.17	15456.320830	EW	...
AST64135	10:58:22.88	-61:46:07.3	13.56	0.92	1.063877940 (74)	0.83	0.05	15456.558135	EW PER	...
AST64136	10:58:38.41	-62:35:30.6	13.87	0.73	0.05	...	VAR	...
AST64197	10:58:39.30	-62:31:33.6	15.84	0.80	0.263724029 (6)	2.29	0.18	15455.719268	EW DS	...
AST64296	10:58:45.02	-62:55:40.3	13.65	1.29	0.08	...	VAR	...
AST64308	10:58:21.57	-61:31:32.5	12.88	1.04	0.07	...	VAR	[G]
AST64442	10:58:33.50	-62:11:52.4	12.96	0.74	0.05	...	VAR	...
AST64493	10:58:17.04	-61:02:46.0	14.75	1.45	3.134212017 (93)	2.97	0.38	15459.931182	EA	...
AST64778	10:58:17.69	-61:12:03.5	12.31	2.84	1.359030247 (59)	0.31	0.11	15456.825713	EW	[G]
AST64879	10:58:16.53	-60:51:49.7	14.92	1.14	0.991783977 (41)	1.65	0.12	15455.914580	PER	...
AST65112	10:58:44.85	-62:26:11.2	15.47	0.75	0.771312177 (81)	0.66	0.12	15456.442901	PER	...
AST65308	10:58:12.35	-60:17:56.6	15.34	1.20	0.704288244 (31)	1.03	0.16	15456.180205	EW PER	...
AST65568	10:58:40.30	-62:06:11.2	13.03	1.96	0.09	...	VAR	...
AST65679	10:58:38.30	-61:57:46.2	15.26	1.78	1.004011989 (14)	0.63	0.84	15456.016143	EA	[A,O]
AST66017	10:58:44.06	-62:08:05.9	13.10	0.89	0.834789872 (50)	0.71	0.05	15455.778838	GD	[G]
AST66226	10:58:18.58	-60:19:58.9	15.42	2.87	0.442695051 (7)	0.94	0.33	15456.066924	EW	[A,O]
AST67325	10:58:34.13	-61:01:53.2	13.64	1.93	0.610230863 (12)	0.34	0.17	15455.755401	EA	[A,O,G]
AST67331	10:58:36.28	-61:10:26.2	12.56	1.74	3.900000095 (135)	0.32	0.18	15459.605010	EA	...
AST67468	10:58:30.09	-60:32:22.9	15.30	2.14	0.34	...	VAR	...
AST67489	10:58:54.17	-61:59:25.5	15.63	2.10	0.636152804 (16)	0.69	0.34	15455.945830	EW	...
AST67652	10:58:24.15	-60:07:15.5	15.17	2.65	1.036239028 (26)	0.59	0.35	15455.793487	EA	...
AST67686	10:58:31.23	-60:41:12.8	13.44	1.34	0.074568003 (1)	2.20	0.05	15455.653838	DS	[G]
AST67750	10:58:25.08	-60:08:33.9	14.96	0.74	0.948569000 (65)	0.49	0.10	15455.770049	EW PER	...
AST67860	10:59:01.97	-62:19:44.3	14.70	0.69	0.182973012 (6)	0.85	0.06	15455.636260	DS	...
AST67933	10:58:42.38	-61:15:34.9	13.45	1.03	4.946595669 (931)	0.31	0.06	15459.415557	PER	...
AST68291	10:59:13.98	-62:45:09.4	15.32	0.65	2.234649181 (98)	0.52	0.49	15456.987823	EA	...
AST68688	10:58:48.67	-61:19:55.2	15.74	1.12	0.62	...	VAR	[G]
AST68860	10:58:46.32	-60:55:09.8	15.45	2.02	2.006680012 (50)	0.89	0.46	15456.698760	EA	[A,O]
AST69102	10:58:44.66	-60:55:31.6	12.93	1.41	0.09	...	VAR	...
AST69131	10:59:05.65	-62:00:01.9	15.26	0.92	1.385008097 (43)	0.89	0.38	15456.710479	EA	...
AST69265	10:58:49.45	-61:02:29.8	14.02	2.87	0.21	...	VAR	[G]
AST69401	10:59:21.34	-62:43:29.4	15.41	5.26	2.956250906 (147)	0.45	0.76	...	DCEP	[G]
AST69426	10:59:15.36	-62:22:21.5	15.41	0.69	0.17	...	VAR	...
AST69676	10:59:07.62	-62:01:41.2	12.36	1.11	1.261240005 (13)	0.44	0.28	15457.034698	EA	[G]
AST69793	10:59:07.83	-61:49:59.5	15.06	0.80	2.676496267 (311)	1.17	0.08	...	MP	...

TABLE 2 — *Continued*

(1) ID	(2) R.A.	(3) Dec.	(4) i (mag ^a)	(5) L	(6) Period ^b (d)	(7) χ^2	(8) Amp (mag)	(9) T_0^c	(10) Type ^d	(11) Note ^e
AST69949	10:59:03.33	-61:30:35.9	15.39	1.27	0.572337806 (20)	0.62	0.19	15456.501495	EW-OC	...
AST69995	10:58:54.87	-61:01:25.3	15.35	3.10	1.225924969 (26)	0.97	0.59	15456.688995	EW	[A,O]
AST70007	10:59:18.62	-62:23:09.4	15.01	1.35	0.15	...	VAR	[G]
AST70054	10:58:48.54	-60:46:17.8	13.61	0.92	0.273245960 (5)	2.25	0.05	15455.725127	EW-OC PER	[A,O]
AST70649	10:59:24.20	-62:24:33.8	14.24	1.52	0.506746173 (27)	0.65	0.09	15456.332549	PER	...
AST70793	10:59:26.05	-62:32:00.5	14.27	2.10	1.428078413 (36)	0.38	0.23	15457.138213	EA	[G]
AST70874	10:59:18.96	-61:58:23.2	15.81	0.75	0.555686116 (31)	0.64	0.14	15455.927276	EW PER	...
AST70909	10:58:54.34	-60:38:43.5	13.42	0.78	0.06	...	VAR	...
AST70929	10:58:49.26	-60:12:05.6	15.95	1.29	0.525443792 (14)	1.54	0.27	15455.882354	EW PER	...
AST71022	10:58:55.24	-60:51:36.5	11.85	6.56	1.059298992 (19)	0.40	0.33	15456.752471	EB	[G]
AST71042	10:59:07.55	-61:46:57.3	12.49	1.37	0.11	...	VAR	...
AST71082	10:59:22.25	-62:19:28.9	13.33	0.68	0.04	...	VAR	...
AST71296	10:59:12.74	-61:30:21.3	13.96	2.05	0.783400357 (27)	1.94	0.14	15455.841338	EW PER	...
AST71576	10:58:56.67	-60:25:15.6	15.19	2.71	0.405622095 (6)	1.67	0.27	15455.989776	EW	[A,O]
AST71613	10:59:09.25	-61:17:26.9	12.85	1.39	0.10	...	VAR	...
AST72114	10:59:06.23	-60:51:27.6	14.28	0.98	0.09	...	VAR	...
AST72125	10:58:52.90	-60:05:05.2	15.15	0.66	1.537524700 (56)	0.66	0.25	15455.905791	EA	...
AST72278	10:58:54.88	-60:10:41.3	13.76	2.18	1.634567142 (20)	1.00	0.49	15456.992705	EA	[G]
AST72361	10:58:55.93	-60:05:03.7	15.86	1.12	3.749475718 (172)	2.15	0.94	15459.315666	EA	...
AST72757	10:59:41.90	-62:33:32.8	13.77	1.87	0.15	...	VAR	...
AST72785	10:59:36.22	-62:16:56.4	15.31	2.67	0.581168115 (9)	0.83	0.35	15456.147979	EW	...
AST73021	10:59:42.09	-62:32:01.4	15.38	1.78	0.372183055 (8)	0.53	0.19	15455.868682	EW	...
AST73109	10:59:35.74	-62:01:09.2	15.67	1.63	0.902405977 (45)	0.69	0.25	15456.601104	EW	...
AST73146	10:59:33.98	-61:54:47.8	15.63	1.23	1.436450005 (69)	3.15	0.37	15456.118682	EB PER	[A,O]
AST73556	10:59:41.98	-62:13:24.4	14.76	1.29	0.10	...	VAR	...
AST73648	10:59:04.92	-60:16:43.9	11.37	2.66	5.383046150 (1236)	0.03	0.36	15460.509307	DCEP	[A]
AST74215	10:59:32.41	-61:33:05.9	13.20	5.27	0.946877956 (15)	0.40	0.23	15456.802276	EW-OC	...
AST74334	10:59:12.06	-60:18:42.4	12.79	13.62	5.380424023 (272)	2.24	0.45	15459.911651	DCEP	[A]
AST74335	10:59:27.91	-61:11:45.1	14.64	1.50	1.281070471 (106)	1.57	0.14	15456.590362	MP	...
AST74404	10:59:22.21	-60:46:59.1	15.00	2.01	1.661826730 (23)	0.61	1.08	15457.099151	EA	[A,O,G]
AST74606	10:59:31.73	-61:17:20.9	15.39	1.05	1.356480002 (55)	0.50	0.27	15457.855010	EA	[A,O]
AST74652	10:59:18.03	-60:30:03.9	15.83	0.99	0.663666129 (13)	1.10	0.39	15456.587432	EA	[A,O]
AST75041	10:59:25.59	-60:48:23.4	14.35	1.33	5.010527134 (89)	2.94	0.41	15456.905791	EA	...
AST75065	10:59:46.52	-61:58:04.4	13.14	0.71	1.726010919 (350)	0.38	0.04	...	PER	...
AST75081	10:59:28.12	-60:53:34.7	14.59	0.78	0.09	...	VAR	[G]
AST75217	11:00:03.51	-62:44:31.6	14.21	0.80	0.06	...	VAR	...
AST75327	10:59:14.14	-60:13:31.0	11.72	0.92	0.14	...	VAR	[G]
AST75336	10:59:23.03	-60:27:49.8	15.47	0.71	1.818343401 (316)	0.50	0.12	...	PER	...
AST75400	10:59:54.50	-62:19:13.8	13.66	0.97	0.08	...	VAR	...
AST75631	10:59:44.08	-61:46:59.2	12.28	1.25	4.403527737 (1353)	0.22	0.07	...	PER	...
AST75636	10:59:46.01	-61:41:53.0	13.93	1.34	0.08	...	VAR	...
AST75743	10:59:28.26	-60:41:10.6	14.08	0.66	1.135247707 (124)	0.75	0.05	15456.100127	EW PER	...
AST75921	10:59:35.66	-60:59:48.7	15.46	1.38	0.397131979 (9)	0.88	0.21	15455.820830	EW	[A,O]
AST75983	10:59:31.37	-60:47:11.5	13.59	0.82	0.06	...	VAR	...
AST76094	11:00:13.31	-62:57:25.1	14.00	0.83	0.06	...	VAR	...
AST76234	10:59:51.04	-61:46:23.5	13.62	1.42	3.231553078 (327)	0.48	0.10	...	MP	...
AST76237	10:59:37.57	-60:56:14.0	15.46	1.37	0.424853921 (12)	0.94	0.16	15456.000518	EW	[A,O]
AST76408	10:59:56.46	-62:02:30.9	13.80	1.38	1.611443520 (45)	2.21	0.17	15457.196807	EA	...
AST76422	10:59:38.62	-61:15:35.8	11.64	0.71	1.512575626 (94)	0.07	0.13	15455.931182	EA	[G]
AST76867	10:59:35.63	-60:41:39.5	13.33	0.91	0.05	...	VAR	[G]
AST76928	10:59:32.47	-60:26:20.2	15.14	0.87	0.09	...	VAR	...
AST77152	10:59:54.59	-61:35:15.8	14.22	1.20	2.358073950 (78)	0.39	0.49	15456.473174	EA	[A,O,G]
AST77247	10:59:58.11	-61:50:12.8	14.43	4.70	0.472918957 (4)	2.31	0.32	15456.147002	EW-OC	[A,O]
AST77535	11:00:21.46	-62:47:46.5	14.71	5.56	0.418929994 (3)	0.54	0.39	15455.815948	EW	[G]
AST77543	10:59:45.44	-60:58:34.9	14.16	0.92	0.08	...	VAR	...
AST77614	10:59:55.18	-61:28:37.8	13.94	1.36	1.693002820 (18)	1.45	0.49	15457.791534	EA	[G]
AST77732	10:59:31.39	-60:09:01.2	15.62	0.86	0.455402941 (12)	1.30	0.36	15456.125518	EB	...
AST78181	10:59:35.61	-60:16:39.1	14.15	0.82	0.06	...	VAR	[G]
AST78295	11:00:26.24	-62:57:43.9	11.82	0.95	2.498666763 (398)	0.10	0.12	15458.425323	EB	[G]
AST78364	10:59:56.42	-61:17:25.3	13.87	1.43	2.577502012 (89)	2.94	0.23	15457.371612	EA	...
AST78612	11:00:04.03	-61:35:18.0	14.68	0.66	0.10	...	VAR	...
AST79050	10:59:59.52	-61:06:51.2	15.48	1.75	3.651263952 (155)	0.55	0.64	15460.842315	EA	...
AST79599	10:59:50.89	-60:36:45.1	15.27	1.02	1.376046419 (178)	0.82	0.14	15456.682159	PER	...
AST79613	10:59:43.56	-60:13:36.8	12.39	1.46	0.07	...	VAR	...
AST79622	11:00:06.47	-61:26:30.1	13.26	1.02	5.061350822 (627)	0.38	0.08	15459.654815	MP?	...
AST79649	10:59:57.83	-60:54:31.6	13.77	1.74	1.137414455 (28)	0.62	0.19	15456.239776	EA	...
AST79966	10:59:46.88	-60:15:55.5	13.34	6.82	2.232448101 (70)	0.46	0.27	15457.567901	EW	[G]
AST80012	11:00:22.62	-62:04:26.2	13.46	1.04	0.06	...	VAR	...
AST80203	11:00:03.69	-61:13:57.1	11.85	0.80	0.08	...	VAR	[G]
AST80240	11:00:18.75	-61:43:17.1	15.86	1.32	0.427687973 (9)	0.91	0.42	15456.019073	EB	...
AST80312	11:00:08.04	-61:13:37.0	12.87	1.50	0.10	...	VAR	[G]
AST80978	11:00:48.71	-62:50:48.4	15.81	0.66	0.350737929 (13)	0.68	0.14	15455.898955	DS EW	...
AST80979	11:00:00.22	-60:26:29.2	15.88	2.50	1.307191014 (34)	2.49	0.77	15456.734893	EA	...

TABLE 2 — *Continued*

(1) ID	(2) R.A.	(3) Dec.	(4) i (mag ^a)	(5) L	(6) Period ^b (d)	(7) χ^2	(8) Amp (mag)	(9) T_0^c	(10) Type ^d	(11) Note ^e
AST81000	11:00:28.38	-62:02:46.4	14.13	1.21	1.654411435 (226)	0.40	0.10	15457.108916	PER	...
AST81429	11:00:04.29	-60:31:35.1	15.11	1.06	0.658730805 (29)	1.16	0.12	15455.999541	EW	...
AST81601	11:00:25.68	-61:33:32.7	15.53	2.82	0.335701942 (2)	2.28	0.71	15455.838409	EW-OC	...
AST81713	11:00:25.74	-61:46:43.9	13.30	1.05	0.07	...	VAR	...
AST81880	11:00:36.34	-61:56:54.0	15.97	1.18	1.182840943 (88)	0.56	0.31	15456.383330	EW	[A,O]
AST82234	11:00:07.40	-60:22:03.5	15.54	1.15	0.346008927 (9)	1.09	0.17	15455.773955	EW	...
AST82352	11:00:21.51	-61:03:50.4	15.99	0.88	2.598101139 (161)	1.06	0.47	15458.010284	EA	...
AST82464	11:00:19.71	-60:56:43.0	15.38	3.72	0.461488903 (6)	0.58	0.40	15456.141143	EW	...
AST82900	11:00:57.73	-62:37:16.4	16.01	1.92	0.378636062 (4)	0.78	0.52	15455.897979	EW	...
AST82902	11:00:15.68	-60:38:05.6	13.45	0.71	1.196163774 (111)	0.34	0.05	15455.955314	PER EW	[G]
AST83207	11:00:27.91	-61:08:29.8	14.09	1.50	2.121176004 (60)	1.67	0.18	...	EA	...
AST83522	11:00:35.59	-61:29:12.5	13.81	2.85	0.19	...	VAR	...
AST83717	11:00:25.06	-60:59:35.5	11.99	6.70	0.53	...	VAR	[A,G]
AST83767	11:00:48.81	-62:00:58.9	13.18	1.18	1.043633938 (64)	0.45	0.06	15456.513213	PER EW	...
AST83801	11:00:36.74	-61:18:14.7	14.92	2.65	0.848176777 (22)	0.43	0.26	15455.955596	EW	...
AST84036	11:01:03.99	-62:36:29.7	14.41	8.58	0.419048011 (2)	0.69	0.62	15455.631377	EW	[G]
AST84135	11:00:23.46	-60:36:15.1	13.98	0.80	0.630318224 (14)	0.34	0.14	15455.978057	EA	...
AST84533	11:00:20.08	-60:15:19.2	13.49	2.37	3.063382864 (491)	0.35	0.10	...	PER	...
AST84604	11:00:48.45	-61:37:49.5	14.14	1.43	4.781635761 (90)	2.11	0.36	15460.908721	EA	...
AST84689	11:00:21.37	-60:18:14.9	13.20	0.81	0.06	...	VAR	[G]
AST84695	11:00:56.82	-62:04:45.3	13.02	1.21	0.07	...	VAR	[G]
AST84931	11:01:04.37	-62:12:53.3	15.71	1.01	2.092283964 (180)	0.60	0.23	15457.631377	EA	...
AST84977	11:00:28.77	-60:44:18.2	12.76	0.72	0.05	...	VAR	...
AST85100	11:00:40.12	-61:06:06.0	13.58	1.40	4.323956013 (602)	0.41	0.10	15456.975127	MP	...
AST85302	11:00:22.82	-60:05:36.8	13.56	1.77	2.960293055 (117)	0.35	0.22	15458.518096	EA	[G]
AST85799	11:01:17.62	-62:32:26.0	13.97	1.62	0.13	...	VAR	...
AST85880	11:00:55.46	-61:28:50.4	15.11	2.47	0.589543819 (12)	4.42	0.36	15456.180205	EW-OC	...
AST85912	11:00:24.20	-60:06:16.0	11.98	6.61	6.132975101 (235)	0.22	0.45	15461.849151	EA EB	[G]
AST85934	11:00:45.32	-60:57:46.1	15.55	1.44	1.390612960 (37)	0.77	0.62	15456.724151	EA EB	[G]
AST85999	11:00:33.03	-60:20:23.0	14.72	0.81	1.135742188 (31)	0.77	0.30	15456.638213	EA	...
AST86485	11:00:47.01	-60:54:29.0	13.87	0.65	1.391839862 (28)	0.52	0.17	15456.886260	EA	...
AST86847	11:01:15.93	-62:05:31.7	16.01	1.03	0.523865879 (19)	1.43	0.32	15455.728057	EW	[A,O]
AST86876	11:01:02.69	-61:33:24.4	13.33	0.68	0.06	...	VAR	...
AST86951	11:01:11.19	-61:49:25.6	14.80	0.77	3.116760015 (138)	0.40	0.19	15457.280791	EA	[A,O]
AST87007	11:01:10.09	-61:45:06.0	14.35	1.16	0.894828022 (54)	0.50	0.08	15455.730987	EW PER	...
AST87126	11:01:04.90	-61:31:24.8	14.09	1.43	0.09	...	VAR	...
AST87214	11:01:07.05	-61:37:16.4	14.52	5.04	0.628040135 (7)	1.01	0.29	15455.646026	EW	[A,O,G]
AST87272	11:01:03.89	-61:27:52.2	13.58	2.33	0.14	...	VAR	...
AST87412	11:00:57.33	-61:03:50.7	15.41	1.13	3.134212255 (270)	0.54	0.28	15456.805205	EA	...
AST87507	11:01:12.77	-61:45:18.0	13.62	0.81	0.06	...	VAR	[G]
AST87739	11:01:23.99	-62:09:42.8	14.70	2.66	1.090512872 (11)	0.50	0.07	...	EA	...
AST87765	11:01:11.67	-61:36:08.4	15.46	1.36	0.318134964 (4)	0.97	0.24	15455.766143	EW	[A,O]
AST88288	11:01:28.49	-62:10:59.4	15.99	0.72	0.847743869 (55)	0.49	0.24	15456.183135	EB EW	...
AST88311	11:00:47.08	-60:12:13.9	14.40	2.67	0.25	...	VAR	...
AST88807	11:01:03.60	-60:53:01.3	12.58	1.18	1.084530234 (62)	0.45	0.07	15456.626495	EW PER	...
AST88839	11:01:25.78	-61:53:17.4	14.14	3.33	0.768816769 (11)	0.34	0.31	15455.693877	EA EB	[A,O,G]
AST88906	11:01:39.33	-62:24:21.0	15.70	0.78	0.602456033 (24)	0.46	0.18	15455.740470	EW	...
AST88907	11:01:38.41	-62:22:06.3	15.04	0.74	0.07	...	VAR	...
AST88908	11:01:02.96	-61:01:10.0	12.28	10.25	2.062977076 (30)	1.01	0.33	15456.743682	EW	[G]
AST88926	11:01:26.96	-61:51:02.2	15.50	1.63	0.21	...	VAR	...
AST89238	11:01:28.67	-61:48:29.1	15.25	0.82	0.931394637 (39)	0.52	0.17	15456.854034	EA EB	[A,O]
AST89418	11:01:27.22	-61:40:52.8	15.52	0.71	1.501621485 (189)	0.46	0.11	15456.966338	PER	...
AST89420	11:01:43.67	-62:26:35.8	15.09	0.66	0.385253936 (15)	1.23	0.08	15456.133330	PER	...
AST89486	11:01:13.02	-61:03:46.8	14.34	2.11	0.16	...	VAR	...
AST89743	11:01:55.79	-62:54:17.2	14.14	1.24	0.10	...	VAR	...
AST90020	11:01:54.53	-62:44:23.2	14.49	4.54	1.755432963 (26)	0.51	0.51	15457.333526	EA	[G]
AST90055	11:01:03.56	-60:21:31.6	15.78	0.70	0.14	...	VAR	...
AST90095	11:01:34.27	-62:12:36.8	11.87	6.07	0.48	...	VAR	[G]
AST90183	11:01:13.44	-60:59:47.6	12.12	1.06	0.521816909 (19)	1.45	0.07	...	MP	[G]
AST90456	11:01:46.65	-62:17:16.7	13.18	1.76	0.140802026 (2)	0.32	0.08	15455.591338	DS	...
AST90563	11:01:24.69	-61:11:53.9	15.11	1.73	0.24	...	VAR	...
AST90571	11:01:44.12	-62:09:47.6	12.34	1.31	0.15	...	VAR	[G]
AST91731	11:01:58.79	-62:21:02.9	13.33	0.96	1.123609185 (98)	1.81	0.06	...	MP	[G]
AST91879	11:01:12.22	-60:10:58.0	15.88	1.04	1.649948955 (94)	0.71	0.50	15457.482940	EA	...
AST91976	11:01:33.95	-61:10:52.3	14.49	1.13	0.13	...	VAR	[G]
AST92009	11:01:53.88	-62:01:08.9	13.99	0.78	1.272266030 (103)	1.39	0.08	...	MP	...
AST92177	11:01:38.48	-61:20:59.1	13.44	1.89	3.766558409 (180)	0.81	0.20	15457.053252	EA	[G]
AST92210	11:01:33.84	-61:08:57.5	13.48	0.71	4.316951752 (269)	0.59	0.13	15456.715362	EA	...
AST92381	11:01:36.50	-61:12:54.0	12.96	1.62	0.09	...	VAR	[G]
AST92676	11:02:09.35	-62:28:23.8	15.44	1.01	0.332666010 (6)	2.11	0.19	15455.957139	EW-OC PER	...
AST92761	11:01:47.17	-61:31:28.9	12.82	0.71	0.06	...	VAR	...
AST92790	11:01:40.34	-61:09:16.2	14.80	2.52	0.565165877 (10)	2.13	0.21	15455.825398	EW-OC	...
AST92823	11:02:05.15	-62:17:23.6	13.79	5.16	3.523474932 (110)	3.47	0.35	...	MP	...

TABLE 2 — *Continued*

(1) ID	(2) R.A.	(3) Dec.	(4) i (mag ^a)	(5) L	(6) Period ^b (d)	(7) χ^2	(8) Amp (mag)	(9) T_0^c	(10) Type ^d	(11) Note ^e
AST92905	11:02:02.51	-62:05:30.6	14.15	3.03	1.219866037 (16)	0.94	0.48	15456.070601	EA	[A,O,G]
AST93025	11:02:05.11	-62:08:31.4	15.86	0.98	0.675100148 (27)	1.29	0.25	15456.175445	EA PER	...
AST93211	11:01:14.38	-60:06:59.7	10.87	1.05	4.585689545 (942)	0.04	0.51	15460.092315	DCEP	[A,G]
AST93860	11:01:52.42	-61:18:52.1	14.32	0.90	0.08	...	VAR	...
AST94842	11:01:47.64	-60:51:56.1	13.03	5.27	1.297754049 (19)	0.58	0.38	15456.340362	EW	[G]
AST95037	11:02:18.65	-62:01:56.5	15.91	0.70	0.542633057 (26)	0.68	0.40	15456.278090	EA EB	[A,O]
AST95098	11:02:30.59	-62:32:42.0	13.83	1.17	1.436138988 (25)	0.65	0.36	15456.684450	EA	[G]
AST95539	11:01:57.08	-60:55:56.0	15.68	0.77	0.338556021 (7)	0.92	0.42	15455.734506	EB-OC	...
AST96345	11:01:52.59	-60:45:11.2	13.10	1.37	2.746053934 (168)	0.20	0.17	15458.397979	EA	[G]
AST62053	10:58:10.51	-61:54:57.6	12.88	2.99	3.320623636 (67)	0.60	0.70	15458.667510	EA	[A,G]
AST93814	11:01:27.07	-60:26:28.9	10.92	1.47	2.218652010 (98)	0.22	0.73	15457.573760	EA EB	[A,G]

NOTE. — [a] The i -band mean magnitude (not an intensity mean). [b] The median value of the period and its standard deviation in brackets in units of 10^{-9} d via MCMC simulation, when applicable. [c] Epoch of minimum light since 1970-01-01 00:00:00 UTC, if possible. [d] type: VAR, objects with statistically significant variabilities, but not showing periodic behaviours; EW, W Urae Majoris-type binary; EB, β Lyrae-type binary; EA, Algol-type binary; EW-OC, EW binary with O’Connell effect; EB-OC, EB binary with O’Connell effect; DCEP, δ Cephei variable; DS, δ Scuti variable; GD, γ Doradus variable; PER, unclassified periodic; MP, multi-periodic; RRAB, RRab Lyrae variable; RRC, RRC Lyrae variable; the “|” sign, separator of two different alternatives. [e] Note: [A], AAVSO variable; [O], OGLE-III variable; [G], GDS variable.

TABLE 3
DISTRIBUTION OF VARIABLE STAR TYPES

Variable Type	N	%	N(new)
Binaries (EW, EB, EA)	285	50.9	143
Pulsators (DS, GD, DCEP, RRab, RRC)	27	4.8	16
Others (PER, MP, VAR)	248	44.3	180

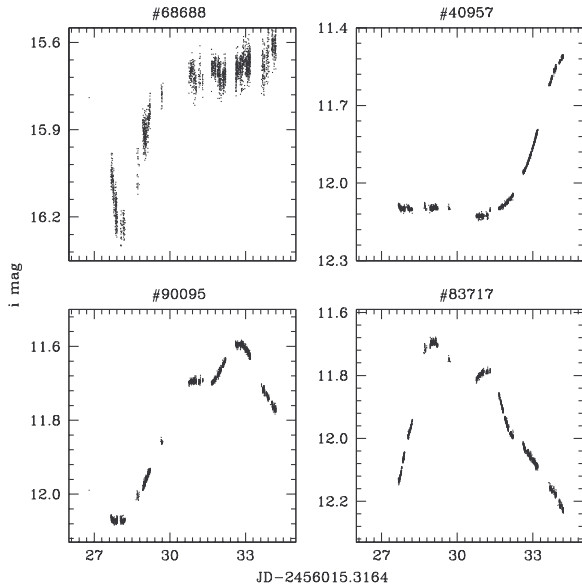


FIG. 9.— Light curves of four unclassified aperiodic variable stars with the largest variability amplitudes.

4. SUMMARY

We have presented the analysis of i band images survey from the AST3-1 telescope towards one Galactic disk field centered at $l = 289.6347^\circ$, $b = -1.5718^\circ$. 560 variable stars were detected in the field from the time series photometry of 92,583 stars with i magnitude ≤ 16.5 mag during the eight days of observations. Multiple methods (LS, BLS, DEBiL and visual inspection) were used to look for the initial periods and we adopted the one that gave the smallest scatter in the phase-folded light curves. We used MCMC simulations based on the harmonic function of the primary period for each variable star to estimate the uncertainty of the period and its median value. For the previously known periodic variable stars, the median periods from the MCMC simulations are highly consistent with those given in the AAVSO database, see Fig. 3.

We tentatively classified the 560 variables into 285 eclipsing binaries (EWs, EBs, EAs), 27 pulsating variable stars (δ Scuti, γ Doradus, δ Cepheid variable and RR Lyrae stars) and 248 other types of variables (unclassified periodic, multi-periodic and aperiodic variable stars). Out of the 560 variables, 339 (61%) are new detections from our data; 42% of the new detections are eclipsing binary stars. We found 34 eclipsing binaries that show O’Connell effects. The interaction between circumstellar matter and the binary components may offer an explanation for the O’Connell effect (see the discussion on AST46538 in §3.2.1). We also found one aperiodic variable that shows a plateau light curve and another one that shows a secondary maximum after peak brightness. Among our newly discovered variables, we found one with complex behaviour showing a binary system with RS CVn-like light curve morphology; we are in the process of obtaining spectroscopic follow-up observations of this object using the Gemini South telescope. All the time-series data of the variable stars will be available via the VizieR Online Data Catalog²².

We thank Márcio Catelan for helpful discussions and Ricardo Salinas when applying for spectral follow-up observations of AST10442. We appreciate comments from the anonymous referees, Lucas Macri for discussions on the Welch-Stetson variability L and Joel Hartman for the discussions on the period uncertainty.

²² <http://vizier.u-strasbg.fr/>

This work was supported by the National Basic Research Program (973 Program) of China (Grant Nos. 2013CB834901, 2013CB834900, 2013CB834903), the Chinese Polar Environment Comprehensive Investigation & Assessment Program (Grand No. CHINARE2016-02-03-05), the National Natural Science Foundation of China (NSFC grants 11303041, 11203039, 11273019, 11273025, 11403048, 11473038, 11673003), the Australian Antarctic Division, and the National Collaborative Research Infrastructure Strategy (NCRIS). LZW acknowledges the Chinese Academy of Sciences (CAS), through a grant to the CAS South America Center for Astronomy (CASSACA) in Santiago, Chile and support by the One-Hundred-Talent program of the Chinese Academy of Sciences (034031001). LFW acknowledges the Strategic Priority Research Program "The

Emergence of Cosmological Structures" of the Chinese Academy of Sciences, Grant No. XDB09000000. JNF acknowledges the support from the Joint Fund of Astronomy of National Natural Science Foundation of China (NSFC) and Chinese Academy of Sciences through the grant U1231202, the National Basic Research Program of China (973 Program 2014CB845700), and the LAM-OST FELLOWSHIP supported by Special Funding for Advanced Users, budgeted and administrated by Center for Astronomical Mega-Science, Chinese Academy of Sciences (CAMS). The authors deeply appreciate the great efforts made by the 24–32th Dome A expedition teams, who provided invaluable assistance to the astronomers that set up and maintained the AST3 and the PLATO-A system.

REFERENCES

- Aristidi, E., Fossat, E., Agabi, A., et al. 2009, *A&A*, 499, 955
- Ashley, M. C. B. 2013, in *IAU Symposium*, Vol. 288, *Astrophysics from Antarctica*, ed. M. G. Burton, X. Cui, & N. F. H. Tothill, 15–24
- Ashley, M. C. B., Bonner, C. S., Everett, J. R., et al. 2010, in *Proc. SPIE*, Vol. 7735, *Ground-based and Airborne Instrumentation for Astronomy III*, 773540
- Bertin, E. 2006, in *Astronomical Society of the Pacific Conference Series*, Vol. 351, *Astronomical Data Analysis Software and Systems XV*, ed. C. Gabriel, C. Arviset, D. Ponz, & S. Enrique, 112
- Bertin, E., & Arnouts, S. 1996, *A&AS*, 117, 393
- Bonner, C. S., Ashley, M. C. B., Cui, X., et al. 2010, *PASP*, 122, 1122
- Breger, M. 2000, in *Astronomical Society of the Pacific Conference Series*, Vol. 210, *Delta Scuti and Related Stars*, ed. M. Breger & M. Montgomery, 3–+
- Brooks, S. P. 1998, *Journal of the Royal Statistical Society. Series D (The Statistician)*, 47, 69
- Burton, M. G. 2010, *A&A Rev.*, 18, 417
- Burton, M. G., Zheng, J., Mould, J., et al. 2016, *Pub. Astron. Soc. Australia*, 33, e047
- Catelan, M., & Smith, H. A. 2015, *Pulsating Stars (Wiley-VCH)*
- Chapellier, E., Mékarnia, D., Abe, L., et al. 2016, *ApJS*, 226, 21
- Crouzet, N., Guillot, T., Agabi, A., et al. 2010, *A&A*, 511, A36
- Cui, X., Yuan, X., & Gong, X. 2008, in *Society of Photo-Optical Instrumentation Engineers (SPIE) Conference Series*, Vol. 7012, *Society of Photo-Optical Instrumentation Engineers (SPIE) Conference Series*
- Cutri, R. M., Skrutskie, M. F., van Dyk, S., et al. 2003, *VizieR Online Data Catalog*, 2246
- Cuyppers, J., Aerts, C., De Cat, P., et al. 2009, *A&A*, 499, 967
- Devor, J. 2005, *ApJ*, 628, 411
- Ducati, J. R., Bevilacqua, C. M., Rembold, S. B., & Ribeiro, D. 2001, *ApJ*, 558, 309
- Fitzgerald, M. P. 1970, *A&A*, 4, 234
- Fu, J. N., Zong, W. K., Yang, Y., et al. 2014, in *IAU Symposium*, Vol. 301, *IAU Symposium*, ed. J. A. Guzik, W. J. Chaplin, G. Handler, & A. Pigulski, 409–410
- Gaulme, P., McKeever, J., Rawls, M. L., et al. 2013, *ApJ*, 767, 82
- Giordano, C., Vernin, J., Chadid, M., et al. 2012, *PASP*, 124, 494
- Girard, T. M., van Altena, W. F., Zacharias, N., et al. 2011, *AJ*, 142, 15
- Gong, X., Wang, L., Cui, X., et al. 2010, in *EAS Publications Series*, Vol. 40, *EAS Publications Series*, ed. L. Spinoglio & N. Epchtein, 65–72
- Hackstein, M., Fein, C., Haas, M., et al. 2015, *Astronomische Nachrichten*, 336, 590
- Hartman, J. D., & Bakos, G. Á. 2016, *ArXiv e-prints*, arXiv:1605.06811
- Hartman, J. D., Gaudi, B. S., Holman, M. J., et al. 2008, *ApJ*, 675, 1254
- Henden, A. A., Templeton, M., Terrell, D., et al. 2016, *VizieR Online Data Catalog*, 2336
- Hu, Y., Shang, Z., Ashley, M. C. B., et al. 2014, *PASP*, 126, 868
- Huang, Z., Fu, J., Zong, W., et al. 2015, *AJ*, 149, 25
- Huang, Z. H., Fu, J. N., & Zong, W. K. 2013, in *EAS Publications Series*, Vol. 64, *EAS Publications Series*, ed. K. Pavlovski, A. Tkachenko, & G. Torres, 401–402
- Jia, P., & Zhang, S. 2012, in *Proc. SPIE*, Vol. 8447, *Adaptive Optics Systems III*, 84475J
- Jia, P., & Zhang, S. 2013, *Research in Astronomy and Astrophysics*, 13, 875
- Kaluzny, J., Stanek, K. Z., Krockenberger, M., et al. 1998, *AJ*, 115, 1016
- Keller, S. C., Schmidt, B. P., Bessell, M. S., et al. 2007, *Pub. Astron. Soc. Australia*, 24, 1
- Kolbas, V., Pavlovski, K., Southworth, J., et al. 2015, *MNRAS*, 451, 4150
- Kovács, G., Zucker, S., & Mazeh, T. 2002, *A&A*, 391, 369
- Krishna Swamy, K. S. 1996, *Astrophysics: a modern perspective (New Age Internat. Publ.)*, 342
- Kulesa, C. A., Walker, C. K., Schein, M., et al. 2008, in *Proc. SPIE*, Vol. 7012, *Ground-based and Airborne Telescopes II*, 701249
- Lascaux, F., Masciadri, E., & Hagelin, S. 2011, *MNRAS*, 411, 693
- Law, N. M., Kulkarni, S. R., Dekany, R. G., et al. 2009, *PASP*, 121, 1395
- Lawrence, J. S., Ashley, M. C. B., Hengst, S., et al. 2009, *Review of Scientific Instruments*, 80, 064501
- Lawrence, J. S., Ashley, M. C. B., Tokovinin, A., & Travouillon, T. 2004, *Nature*, 431, 278
- Lawrence, J. S., Ashley, M. C. B., Burton, M. G., et al. 2006, in *Proc. SPIE*, Vol. 6267, *Society of Photo-Optical Instrumentation Engineers (SPIE) Conference Series*, 62671L
- Lawrence, J. S., Allen, G. R., Ashley, M. C. B., et al. 2008, in *Proc. SPIE*, Vol. 7012, *Ground-based and Airborne Telescopes II*, 701227
- Li, X., Wang, D., Xu, L., et al. 2012a, in *Proc. SPIE*, Vol. 8444, *Ground-based and Airborne Telescopes IV*, 84445M
- Li, Y., Zheng, J., Tuthill, P., et al. 2016, *Pub. Astron. Soc. Australia*, 33, e008
- Li, Z., Yuan, X., Cui, X., et al. 2012b, in *Proc. SPIE*, Vol. 8444, *Ground-based and Airborne Telescopes IV*, 84441O
- Liang, E.-S., Wang, S., Zhou, J.-L., et al. 2016, *ArXiv e-prints*, arXiv:1608.07904
- Liu, Q.-Y., & Yang, Y.-L. 2003, *Chin. J. Astron. Astrophys.*, 3, 142
- Lomb, N. R. 1976, *Ap&SS*, 39, 447
- LSST Science Collaboration, Abell, P. A., Allison, J., et al. 2009, *ArXiv e-prints*, arXiv:0912.0201
- Ma, B., Shang, Z., Hu, Y., et al. 2014, in *Society of Photo-Optical Instrumentation Engineers (SPIE) Conference Series*, Vol. 9154, *Society of Photo-Optical Instrumentation Engineers (SPIE) Conference Series*, 1
- Ma, B., Shang, Z., Wang, L., et al. 2012, in *Society of Photo-Optical Instrumentation Engineers (SPIE) Conference Series*, Vol. 8446, *Society of Photo-Optical Instrumentation Engineers (SPIE) Conference Series*, 6

- Mékarnia, D., Guillot, T., Rivet, J.-P., et al. 2016, *MNRAS*, 463, 45
- Meng, Z., Zhou, X., Zhang, H., et al. 2013, *PASP*, 125, 1015
- Milone, E. E. 1968, *AJ*, 73, 708
- Moore, A., Allen, G., Aristidi, E., et al. 2008, in *Proc. SPIE*, Vol. 7012, *Ground-based and Airborne Telescopes II*, 701226
- Nataf, D. M., Stanek, K. Z., & Bakos, G. Á. 2010, *Acta Astronomica*, 60, 261
- O’Connell, D. J. K. 1951, *Publications of the Riverview College Observatory*, 2, 85
- Oelkers, R. J., Macri, L. M., Wang, L., et al. 2015, *AJ*, 149, 50 —. 2016, *AJ*, 151, 166
- Pei, C., Yuan, X. Y., Chen, H. L., et al. 2011, *Acta Astronomica Sinica*, 52, 401
- Pei, C., Yuan, X.-Y., Chen, H.-L., et al. 2012, *Chinese Astron. Astrophys.*, 36, 327
- Pietrukowicz, P., Mróz, P., Soszyński, I., et al. 2013, *Acta Astronomica*, 63, 115
- Pojmanski, G. 2005, *VizieR On-line Data Catalog: J/other/AcA/50.177*. Originally published in: 2000AcA....50..177P, 50, 5001
- Qian, S.-B., Wang, J.-J., Zhu, L.-Y., et al. 2014, *ApJS*, 212, 4
- Rau, A., Kulkarni, S. R., Law, N. M., et al. 2009, *PASP*, 121, 1334
- Röser, S., Schilbach, E., Schwan, H., et al. 2008, *A&A*, 488, 401
- Samus, N. N., Durlevich, O. V., & et al. 2009, *VizieR Online Data Catalog*, 1, 2025
- Scargle, J. D. 1982, *ApJ*, 263, 835
- Schmidt, E. G., Johnston, D., Langan, S., & Lee, K. M. 2004, *AJ*, 128, 1748
- Shang, Z., Hu, K., Hu, Y., et al. 2012, in *Society of Photo-Optical Instrumentation Engineers (SPIE) Conference Series*, Vol. 8448, *Society of Photo-Optical Instrumentation Engineers (SPIE) Conference Series*, 26
- Sims, G., Ashley, M. C. B., Cui, X., et al. 2010, in *Proc. SPIE*, Vol. 7733, *Ground-based and Airborne Telescopes III*, 77334M
- Sims, G., Ashley, M. C. B., Cui, X., et al. 2012a, *PASP*, 124, 637 —. 2012b, *PASP*, 124, 74
- Smith, H. A. 2004, *RR Lyrae Stars* (Cambridge University Press), 166
- Soderhjelm, S. 1980, *A&A*, 89, 100
- Soszyński, I., Poleski, R., Udalski, A., et al. 2008, *Acta Astronomica*, 58, 163
- Soszyński, I., Udalski, A., Szymański, M. K., et al. 2008, *Acta Astronomica*, 58, 293
- Stetson, P. B. 1996, *PASP*, 108, 851
- Storey, J. W. V. 2013, in *IAU Symposium*, Vol. 288, *IAU Symposium*, ed. M. G. Burton, X. Cui, & N. F. H. Tothill, 1–5
- Tothill, N. F. H., Kulesa, C. A., Walker, C. K., et al. 2008, in *EAS Publications Series*, Vol. 33, *EAS Publications Series*, ed. H. Zinnecker, N. Epchtein, & H. Rauer, 301–306
- Tremblin, P., Minier, V., Schneider, N., et al. 2011, *A&A*, 535, A112
- Wang, L., Macri, L. M., Krisciunas, K., et al. 2011, *AJ*, 142, 155
- Wang, L., Macri, L. M., Wang, L., et al. 2013a, *AJ*, 146, 139
- Wang, L., Macri, L. M., Wang, L., et al. 2013b, in *IAU Symposium*, Vol. 288, *Astrophysics from Antarctica*, ed. M. G. Burton, X. Cui, & N. F. H. Tothill, 320–321
- Wang, S., Zhou, X., Zhang, H., et al. 2012, *PASP*, 124, 1167
- Wang, S., Zhang, H., Zhou, J.-L., et al. 2014a, *ApJS*, 211, 26
- Wang, S., Zhang, H., Zhou, X., et al. 2015, *ApJS*, 218, 20
- Wang, S.-H., Zhou, X., Zhang, H., et al. 2014b, *Research in Astronomy and Astrophysics*, 14, 345
- Watson, C., Henden, A. A., & Price, A. 2016, *VizieR Online Data Catalog*, 1
- Wei, P., Shang, Z., Ma, B., et al. 2014, in *Society of Photo-Optical Instrumentation Engineers (SPIE) Conference Series*, Vol. 9149, *Society of Photo-Optical Instrumentation Engineers (SPIE) Conference Series*, 2
- Welch, D. L., & Stetson, P. B. 1993, *AJ*, 105, 1813
- Wen, H., Gong, X., & Zhang, R. 2012, in *Proc. SPIE*, Vol. 8444, *Ground-based and Airborne Telescopes IV*, 84445F
- Xu, J., Gong, X., & Gu, B. 2016, *PASP*, 128, 125004
- Xu, L. 2012, in *Proc. SPIE*, Vol. 8451, *Software and Cyberinfrastructure for Astronomy II*, 845114
- Yang, H., Allen, G., Ashley, M. C. B., et al. 2009, *PASP*, 121, 174
- Yang, H., Kulesa, C. A., Walker, C. K., et al. 2010, *PASP*, 122, 490
- Yang, M., Zhang, H., Wang, S., et al. 2015, *ApJS*, 217, 28
- Yang, Y., Moore, A. M., Krisciunas, K., et al. 2016, *ArXiv e-prints*, arXiv:1610.10094
- Yao, X., Wang, L., Wang, X., et al. 2015, *AJ*, 150, 107
- Yuan, X., Cui, X., Su, D.-q., et al. 2013, in *IAU Symposium*, Vol. 288, *IAU Symposium*, ed. M. G. Burton, X. Cui, & N. F. H. Tothill, 271–274
- Yuan, X., & Su, D.-q. 2012, *MNRAS*, 424, 23
- Yuan, X., Cui, X., Liu, G., et al. 2008, in *Society of Photo-Optical Instrumentation Engineers (SPIE) Conference Series*, Vol. 7012, *Society of Photo-Optical Instrumentation Engineers (SPIE) Conference Series*
- Yuan, X., Cui, X., Gu, B., et al. 2014, in *Society of Photo-Optical Instrumentation Engineers (SPIE) Conference Series*, Vol. 9145, *Society of Photo-Optical Instrumentation Engineers (SPIE) Conference Series*, 0
- Yuan, X., Cui, X., Wang, L., et al. 2015, *IAU General Assembly*, 22, 56923
- Zacharias, N., Finch, C. T., Girard, T. M., et al. 2013, *AJ*, 145, 44
- Zhou, X., Wu, Z., Jiang, Z., et al. 2010a, *Research in Astronomy and Astrophysics*, 10, 279
- Zhou, X., Fan, Z., Jiang, Z., et al. 2010b, *PASP*, 122, 347
- Zhou, X., Ashley, M. C. B., Cui, X., et al. 2013, in *IAU Symposium*, Vol. 288, *Astrophysics from Antarctica*, ed. M. G. Burton, X. Cui, & N. F. H. Tothill, 231–238
- Zhu, Y., Wang, L., Yuan, X., et al. 2014, in *Society of Photo-Optical Instrumentation Engineers (SPIE) Conference Series*, Vol. 9145, *Society of Photo-Optical Instrumentation Engineers (SPIE) Conference Series*, 0
- Zong, W., Fu, J.-N., Niu, J.-S., et al. 2015, *AJ*, 149, 84
- Zou, H., Zhou, X., Jiang, Z., et al. 2010, *AJ*, 140, 602

TABLE 4
IDENTIFICATIONS FOR THE 221 VARIABLES IN COMMON

(1) AST3	(2) AAVSO	(3) GDS	(4) OGLE-III or others
AST01736	...	GDS_J1050304-613526	...
AST02497	310338	...	OGLE-GD-ECL-03652
AST03182	310357	...	OGLE-GD-ECL-03671
AST04554	...	GDS_J1050526-615847	...
AST05016	...	GDS_J1050463-602841	...
AST05512	310418	...	OGLE-GD-ECL-03733
AST06264	310438	GDS_J1051045-612147	OGLE-GD-ECL-03753
AST06935	310450	...	OGLE-GD-ECL-03765
AST07839	...	GDS_J1051142-614524	...
AST08666	92320	GDS_J1051153-603208	ASAS J105115-6032.1
AST10372	...	GDS_J1051315-600945	...
AST11515	...	GDS_J1051453-614613	...
AST11525	310601	GDS_J1051435-610220	OGLE-GD-ECL-03919
AST12715	310634	...	OGLE-GD-ECL-03957
AST13387	5954	GDS_J1051541-612802	GS Car
AST13431	226193	...	[PMF2009] V041
AST13451	310655	...	OGLE-GD-ECL-03980
AST14578	310681	GDS_J1052054-612031	OGLE-GD-ECL-04022
AST15280	...	GDS_J1052104-603541	...
AST16017	...	GDS_J1052179-612010	...
AST16336	...	GDS_J1052096-612546	...
AST16539	226339	GDS_J1052229-613208	[PMF2009] V114
AST16578	...	GDS_J1052152-602413	...
AST16670	...	GDS_J1052165-602348	...
AST16693	...	GDS_J1052219-603335	...
AST17775	358801	...	OGLE-GD-CEP-0005
AST17938	310754	...	OGLE-GD-ECL-04118
AST17970	...	GDS_J1052246-603438	...
AST18900	310774	...	OGLE-GD-ECL-04146
AST19397	...	GDS_J1052465-615633	...
AST19571	310815	GDS_J1052504-615557	OGLE-GD-ECL-04193
AST20003	...	GDS_J1052484-612033	...
AST20657	310822	GDS_J1052518-612125	OGLE-GD-ECL-04200
AST20751	310834	...	OGLE-GD-ECL-04212
AST21008	...	GDS_J1052487-603916	...
AST21898	310869	GDS_J1053033-613822	OGLE-GD-ECL-04249
AST22118	...	GDS_J1053013-610728	...
AST22962	310898	...	OGLE-GD-ECL-04280
AST23445	...	GDS_J1053079-600853	...
AST23515	310915	...	OGLE-GD-ECL-04309
AST23549	...	GDS_J1053169-621112	...
AST23732	...	GDS_J1053269-625034	...
AST24162	...	GDS_J1053208-611234	...
AST24483	310927	GDS_J1053209-605115	OGLE-GD-ECL-04325
AST24595	310958	...	OGLE-GD-ECL-04363
AST24761	...	GDS_J1053314-620336	...
AST24936	...	GDS_J1053343-621959	...
AST25082	...	GDS_J1053201-602952	...
AST25633	...	GDS_J1053332-612915	...
AST25740	226643	...	[PMF2009] V266
AST26037	...	GDS_J1053336-610336	...
AST26542	...	GDS_J1053357-612416	...
AST26602	5982	GDS_J1053415-613654	IL Car
AST27264	...	GDS_J1053355-602114	...
AST27396	311017	GDS_J1053454-611535	OGLE-GD-ECL-04451
AST27446	...	GDS_J1053405-604122	...
AST27616	311038	GDS_J1053518-614300	OGLE-GD-ECL-04478
AST28591	...	GDS_J1053575-614028	...
AST28592	...	GDS_J1053555-612813	...
AST28694	...	GDS_J1053474-603313	...
AST29379	...	GDS_J1053508-601527	...
AST29542	311073	...	OGLE-GD-ECL-04521
AST30846	...	GDS_J1054054-603728	...
AST31492	311144	...	OGLE-GD-ECL-04596
AST31705	311154	...	OGLE-GD-ECL-04606
AST33265	5857	GDS_J1054268-612049	CC Car
AST35554	311250	...	OGLE-GD-ECL-04704
AST35618	...	GDS_J1054426-604647	...
AST36262	...	GDS_J1054491-604040	...
AST37489	311315	...	OGLE-GD-ECL-04769
AST37704	...	GDS_J1055143-623605	...
AST37940	311326	GDS_J1055106-613508	OGLE-GD-ECL-04780
AST38214	...	GDS_J1055183-622619	...
AST38428	...	GDS_J1055119-614224	...
AST38531	311348	...	OGLE-GD-ECL-04803

TABLE 4 — *Continued*

(1) AST3	(2) AAVSO	(3) GDS	(4) OGLE-III or others
AST38989	311335	...	OGLE-GD-ECL-04789
AST39051	...	GDS_J1055164-613623	...
AST39579	311340	...	OGLE-GD-ECL-04794
AST39766	...	GDS_J1055076-600437	...
AST39901	311400	...	OGLE-GD-ECL-04858
AST39979	5983	GDS_J1055097-603251	IM Car
AST40137	...	GDS_J1055312-621143	...
AST40536	311382	GDS_J1055215-605455	OGLE-GD-ECL-04840
AST40655	311441	...	OGLE-GD-ECL-04899
AST40671	311383	GDS_J1055216-605032	OGLE-GD-ECL-04841
AST40766	311387	GDS_J1055231-605051	OGLE-GD-ECL-04845
AST40904	311392	...	OGLE-GD-ECL-04850
AST40957	...	GDS_J1055122-600930	...
AST41209	...	GDS_J1055237-603407	...
AST41484	...	GDS_J1055396-621808	...
AST41594	311497	...	OGLE-GD-ECL-04955
AST41650	...	GDS_J1055417-622358	...
AST41745	311391	...	OGLE-GD-ECL-04849
AST42287	311470	...	OGLE-GD-ECL-04928
AST42633	311469	...	OGLE-GD-ECL-04927
AST42854	...	GDS_J1055451-614004	...
AST42869	311535	...	OGLE-GD-ECL-04993
AST43064	56994	...	NSV 18559
AST43350	311558	...	OGLE-GD-ECL-05017
AST43409	...	GDS_J1055342-600459	...
AST43421	311472	...	OGLE-GD-ECL-04930
AST43594	311494	...	OGLE-GD-ECL-04952
AST43846	...	GDS_J1056058-622946	...
AST44142	311616	GDS_J1056002-615337	OGLE-GD-ECL-05075
AST45236	311601	...	OGLE-GD-ECL-05060
AST45483	311620	...	OGLE-GD-ECL-05079
AST45682	...	GDS_J1055547-603155	...
AST46247	311651	...	OGLE-GD-ECL-05110
AST46538	...	GDS_J1056047-604149	...
AST46624	...	GDS_J1056072-605408	...
AST46738	...	GDS_J1056223-615935	...
AST46971	...	GDS_J1056028-601408	...
AST48664	...	GDS_J1056375-621855	...
AST49035	311772	GDS_J1056276-605613	OGLE-GD-ECL-05232
AST50267	311762	...	OGLE-GD-ECL-05222
AST50549	311789	...	OGLE-GD-ECL-05249
AST50581	...	GDS_J1056268-601705	...
AST51624	311830	GDS_J1056353-601239	OGLE-GD-ECL-05291
AST53357	311884	GDS_J1056468-601442	OGLE-GD-ECL-05346
AST53821	...	GDS_J1056563-604013	...
AST53841	...	GDS_J1057193-623419	...
AST54338	311973	...	OGLE-GD-ECL-05436
AST54349	311929	...	OGLE-GD-ECL-05392
AST54537	311991	GDS_J1057065-610112	OGLE-GD-ECL-05454
AST54590	312031	GDS_J1057151-613403	OGLE-GD-ECL-05494
AST55024	311997	...	OGLE-GD-ECL-05460
AST55167	...	GDS_J1057307-623116	...
AST55334	...	GDS_J1057013-601502	...
AST56058	312096	GDS_J1057298-615200	OGLE-GD-ECL-05560
AST56624	...	GDS_J1057448-623935	...
AST56993	...	GDS_J1057296-613940	...
AST57491	312051	...	OGLE-GD-ECL-05514
AST59186	312200	...	OGLE-GD-ECL-05667
AST59773	312166	...	OGLE-GD-ECL-05632
AST60119	...	GDS_J1057348-602105	...
AST61176	312195	...	OGLE-GD-ECL-05662
AST61299	...	GDS_J1058171-623624	...
AST61514	...	GDS_J1057588-614517	...
AST61607	312291	...	OGLE-GD-ECL-05761
AST61969	312222	GDS_J1057573-605700	OGLE-GD-ECL-05690
AST62053	5772	GDS_J1058105-615457	SS Car
AST62121	312262	GDS_J1058047-612228	OGLE-GD-ECL-05732
AST62331	312278	...	OGLE-GD-ECL-05748
AST62372	312176	GDS_J1057488-601234	OGLE-GD-ECL-05642
AST62838	...	GDS_J1058028-610857	...
AST62877	358849	...	OGLE-GD-RRLYR-0020
AST63063	312274	...	OGLE-GD-ECL-05744
AST63331	312220	...	OGLE-GD-ECL-05688
AST64031	312282	...	OGLE-GD-ECL-05752
AST64308	...	GDS_J1058215-613132	...
AST64778	...	GDS_J1058176-611203	...

TABLE 4 — *Continued*

(1) AST3	(2) AAVSO	(3) GDS	(4) OGLE-III or others
AST65679	312442	...	OGLE-GD-ECL-05913
AST66017	...	GDS_J1058445-620806	...
AST66226	312330	...	OGLE-GD-ECL-05800
AST67325	312421	GDS_J1058341-610153	OGLE-GD-ECL-05892
AST67686	...	GDS_J1058311-604113	...
AST68688	...	GDS_J1058486-611955	...
AST68860	312484	...	OGLE-GD-ECL-05956
AST69265	...	GDS_J1058494-610230	...
AST69401	...	GDS_J1059213-624329	...
AST69676	...	GDS_J1059076-620141	...
AST69995	312533	...	OGLE-GD-ECL-06005
AST70007	...	GDS_J1059186-622309	...
AST70054	312497	...	OGLE-GD-ECL-05969
AST70793	...	GDS_J1059265-623200	...
AST71022	...	GDS_J1058552-605136	...
AST71576	312543	...	OGLE-GD-ECL-06015
AST72278	...	GDS_J1058549-601041	...
AST73146	312755	...	OGLE-GD-ECL-06231
AST73648	5860	...	CF Car
AST74334	6195	...	V0442 Car
AST74404	312671	GDS_J1059222-604659	OGLE-GD-ECL-06146
AST74606	312741	...	OGLE-GD-ECL-06217
AST74652	312651	...	OGLE-GD-ECL-06125
AST75081	...	GDS_J1059281-605335	...
AST75327	...	GDS_J1059141-601331	...
AST75921	312765	...	OGLE-GD-ECL-06242
AST76237	312773	...	OGLE-GD-ECL-06250
AST76422	...	GDS_J1059386-611535	...
AST76867	...	GDS_J1059356-604139	...
AST77152	312841	GDS_J1059546-613515	OGLE-GD-ECL-06321
AST77247	312848	...	OGLE-GD-ECL-06328
AST77535	...	GDS_J1100214-624746	...
AST77614	...	GDS_J1059551-612837	...
AST78181	...	GDS_J1059356-601639	...
AST78295	...	GDS_J1100262-625744	...
AST79966	...	GDS_J1059469-601556	...
AST80203	...	GDS_J1100036-611357	...
AST80312	...	GDS_J1100081-611337	...
AST81880	312869	...	OGLE-GD-ECL-06350
AST82902	...	GDS_J1100156-603805	...
AST83717	5929	GDS_J1100256-605935	FM Car
AST84036	...	GDS_J1101041-623629	...
AST84689	...	GDS_J1100213-601815	...
AST84695	...	GDS_J1100568-620445	...
AST85302	...	GDS_J1100228-600536	...
AST85912	...	GDS_J1100242-600616	...
AST85934	...	GDS_J1100453-605746	...
AST86847	312949	...	OGLE-GD-ECL-06431
AST86951	312942	...	OGLE-GD-ECL-06423
AST87214	312932	GDS_J1101075-613716	OGLE-GD-ECL-06413
AST87507	...	GDS_J1101127-614518	...
AST87765	312943	...	OGLE-GD-ECL-06424
AST88839	312963	GDS_J1101257-615317	OGLE-GD-ECL-06445
AST88908	...	GDS_J1101029-610110	...
AST89238	312970	...	OGLE-GD-ECL-06452
AST90020	...	GDS_J1101545-624423	...
AST90095	...	GDS_J1101342-621237	...
AST90183	...	GDS_J1101134-605947	...
AST90571	...	GDS_J1101441-620947	...
AST91731	...	GDS_J1101588-622103	...
AST91976	...	GDS_J1101339-611052	...
AST92177	...	GDS_J1101385-612058	...
AST92381	...	GDS_J1101365-611253	...
AST92905	313020	GDS_J1102025-620530	OGLE-GD-ECL-06503
AST93211	5930	GDS_J1101143-600659	FN Car
AST93814	5963	GDS_J1101276-602629	HI Car
AST94842	...	GDS_J1101476-605156	...
AST95037	313050	...	OGLE-GD-ECL-06533
AST95098	...	GDS_J1102306-623242	...
AST96345	...	GDS_J1101525-604511	...